# 1 Efficient Inference of Macrophylogenies: Insights from the

# **2** Avian Tree of Life

3

- 4 Min Zhao<sup>1,2,\*,§</sup>, Gregory Thom<sup>3,4,\*</sup>, Brant C. Faircloth<sup>3,4</sup>, Michael J. Andersen<sup>5</sup>, F. Keith Barker<sup>6</sup>,
- 5 Brett W. Benz<sup>7</sup>, Michael J. Braun<sup>8,9</sup>, Gustavo A. Bravo<sup>10,11</sup>, Robb T. Brumfield<sup>3,4</sup>, R. Terry
- 6 Chesser<sup>12,13</sup>, Elizabeth P. Derryberry<sup>14</sup>, Travis C. Glenn<sup>15</sup>, Michael G. Harvey<sup>16</sup>, Peter A. Hosner<sup>17</sup>,
- 7 Tyler S. Imfeld<sup>18</sup>, Leo Joseph<sup>19</sup>, Joseph D. Manthey<sup>20</sup>, John E. McCormack<sup>21</sup>, Jenna M.
- 8 McCullough<sup>5,22</sup>, Robert G. Moyle<sup>23</sup>, Carl H. Oliveros<sup>4</sup>, Noor D. White Carreiro<sup>24</sup>, Kevin Winker<sup>25</sup>,
- 9 Daniel J. Field<sup>26, 27</sup>, Daniel T. Ksepka<sup>28,29</sup>, Edward L. Braun<sup>1,§</sup>, Rebecca T. Kimball<sup>1,§</sup>, Brian Tilston
- 10 Smith<sup>29,§</sup>

11

- 12 \* Contributed equally
- 13 § Corresponding authors (balaenazhao@gmail.com; ebraun68@ufl.edu; rkimball@ufl.edu;
- 14 briantilstonsmith@gmail.com)

15

- 1. Department of Biology, University of Florida, Gainesville, FL 32611, USA
- 17 2. Department of Biological Sciences, Virginia Tech, Blacksburg, VA 24061, USA
- 18 3. Museum of Natural Sciences, Louisiana State University, Baton Rouge, LA 70803, USA
- 4. Department of Biological Sciences, Louisiana State University, Baton Rouge, LA 70803, USA
- 20 5. Department of Biology and Museum of Southwestern Biology, University of New Mexico,
- 21 Albuquerque, NM 87131, USA
- 22 6. Bell Museum of Natural History and Department of Ecology, Evolution and Behavior,
- 23 University of Minnesota, St. Paul, MN 55105, USA
- 7. Department of Ecology and Evolutionary Biology and Museum of Zoology, University of
- 25 Michigan, Ann Arbor, MI 48103, USA
- 26 8.Department of Vertebrate Zoology, National Museum of Natural History, Smithsonian
- 27 Institution; Washington, DC 20013, USA
- 28 9. Department of Biology and Biological Sciences Graduate Program, University of Maryland;
- 29 College Park, MD 20742, USA
- 30 10. Center for Biological Collections and Species Management, Instituto Alexander von
- 31 Humboldt, Villa de Leyva, Colombia
- 32 11. Museum of Comparative Zoology & Department of Organismic and Evolutionary Biology,
- 33 Harvard University, Cambridge, MA 02138, USA

- 34 12. U.S. Geological Survey, Eastern Ecological Science Center, 12100 Beech Forest Road, Laurel,
- 35 MD 20708, USA
- 36 13. Dept. of Vertebrate Zoology, National Museum of Natural History, Smithsonian Institution,
- 37 P.O. Box 37012, Washington, DC 20013-7012, USA
- 38 14. Department of Ecology and Evolutionary Biology, University of Tennessee, Knoxville, TN
- 39 37996, USA
- 40 15. Department of Environmental Health Science and Institute of Bioinformatics, University of
- 41 Georgia, Athens, GA 30602, USA
- 42 16. Department of Biological Sciences and Biodiversity Collections, The University of Texas at El
- 43 Paso, El Paso, TX 79968, USA
- 44 17. Natural History Museum of Denmark and Center for Global Mountain Biodiversity,
- 45 University of Copenhagen, Copenhagen 1172, Denmark
- 46 18. Department of Biology, Xavier University, Cincinnati, OH 45207 USA
- 47 19. Australian National Wildlife Collection, CSIRO National Research Collections Australia,
- 48 Canberra, ACT 2602, Australia
- 49 20. Department of Biological Sciences, Texas Tech University, Lubbock, TX 79409, USA
- 50 21. Moore Laboratory of Zoology, Occidental College, Los Angeles, CA 90041, USA
- 22. Department of Biology, University of Kentucky, Lexington, KY 40506, USA
- 52 23. Department of Ecology and Evolutionary Biology and Biodiversity Institute, University of
- Kansas, Lawrence, KS 66045, USA
- 54 24. Biological Imaging Core, National Eye Institute, National Institutes of Health, Bethesda, MD
- 55 20892, USA
- 56 25. University of Alaska Museum, Fairbanks, AK 99775, USA
- 57 26. Department of Earth Sciences, University of Cambridge, Downing St, Cambridge, CB2 3EQ,
- 58 UK
- 59 27. Museum of Zoology, University of Cambridge, Downing Pl, Cambridge, CB2 3EJ, UK
- 60 28. Bruce Museum, Greenwich, CT 06830, USA
- 61 29. Department of Ornithology, American Museum of Natural History, Central Park West at
- 62 79th Street, New York, NY 10024, USA

63 64

65

#### **Abstract**

- The exponential growth of molecular sequence data over the past decade has enabled the
- 67 construction of numerous clade-specific phylogenies encompassing hundreds or thousands of
- taxa. These independent studies often include overlapping data, presenting a unique
- opportunity to build macrophylogenies (phylogenies sampling > 1,000 taxa) for entire classes
- across the Tree of Life. However, the inference of large trees remains constrained by logistical,
- 71 computational, and methodological challenges. The Avian Tree of Life provides an ideal model

for evaluating strategies to robustly infer macrophylogenies from intersecting datasets derived from smaller studies. In this study, we leveraged a comprehensive resource of sequence capture datasets to evaluate the phylogenetic accuracy and computational costs of four methodological approaches: (1) supermatrix approaches using concatenation, including the "fast" maximum likelihood (ML) methods, (2) filtering datasets to reduce heterogeneity, (3) supertree estimation based on published phylogenomic trees, and (4) a "divide-and-conquer" strategy, wherein smaller ML trees were estimated and subsequently combined using a supertree approach. Additionally, we examined the impact of these methods on divergence time estimation using a dataset that includes newly vetted fossil calibrations for the Avian Tree of Life. Our findings highlight the advantages of recently developed fast tree search approaches initiated with parsimony starting trees, which offer a reasonable compromise between computational efficiency and phylogenetic accuracy, facilitating inference of macrophylogenies.

### **Keywords**

Macrophylogeny, phylogenomics, supermatrix, supertree, ultraconserved elements, birds

### Introduction

Completing the Tree of Life remains a significant bottleneck to addressing a wide range of questions in comparative biology (Cracraft and Donoghue 2004). Advances in sequencing technologies (reviewed by McCormack et al. (2013)), computational methods (e.g., Kozlov et al. 2019), and user-friendly bioinformatic pipelines (e.g., Faircloth 2016) have made the production and analysis of phylogenomic datasets involving hundreds of taxa increasingly routine.

However, scaling these techniques to datasets with thousands of loci and thousands of taxa presents substantial logistical, computational, and methodological challenges (Delsuc et al. 2005; Philippe et al. 2011; Kapli et al. 2020). The construction of such "macrophylogenies" (Title and Rabosky 2017) often relies on combining independently produced datasets, which frequently have limited overlap and substantial missing data (Sanderson et al. 2010).

Past attempts to infer macrophylogenies from independently produced datasets typically used two general approaches: supermatrix and supertree methods. Supermatrix methods infer phylogenies directly from orthologous loci, often compiled from multiple studies. However, these methods are negatively affected by large amounts of missing data (Driskell et al. 2004; Philippe et al. 2004; Goloboff et al. 2009; Hosner et al. 2016) and varying standards of data quality (Philippe et al. 2011). Analyses of supermatrices are also vulnerable to common issues in phylogenetic analyses, such as alignment errors (Ogden and Rosenberg 2006) and the inclusion of non-orthologous sequences (Koonin 2005), which are often exacerbated in supermatrices due to the heterogeneous nature of the data. Additionally, supermatrix methods face escalating computational demands that increase nonlinearly (Bader et al. 2006) as both the width (number of sites) and height (number of taxa) of the matrix expand (Delsuc et al. 2005). Some challenges, such as data quality and alignment issues, can be mitigated to an extent by analyzing multiple datasets filtered to remove "noise" in different ways and comparing the results (Kuhl et al. 2021). However, this approach is limited by the significant computational costs of performing multiple analyses on large datasets. Superfree methods, by contrast, generate phylogenies by combining existing tree topologies (Sanderson et al. 1998; Bininda-Emonds 2004; Cotton and Wilkinson 2009). These methods are more computationally efficient and can effectively incorporate trees built with heterogeneous data (Liu et al. 2001; Hinchliff et al. 2015; Redelings and Holder 2017). However, most supertree methods cannot directly estimate meaningful branch lengths. Despite the strengths and limitations of these methods, rigorous comparisons of the ability of supermatrix and supertree methods to estimate macrophylogenies using phylogenomic data remain rare. This gap largely reflects the limited availability of large-scale genomic datasets for most taxonomic groups.

99

100

101

102

103

104

105

106

107

108

109

110

111

112

113

114

115

116

117

118

119

120

121

122

123

124

125

126

127

Class Aves (birds) is one taxonomic group with sufficient data to perform these types of comparative analyses. As the most species-rich terrestrial vertebrate group, with 11,140 species recognized (Gill et al. 2023), birds have received extensive attention from phylogenetic systematists (e.g., Hackett et al. 2008; Jetz et al. 2012; McCormack et al. 2013; Jarvis et al. 2014; Burleigh et al. 2015; Prum et al. 2015; Moyle et al. 2016; Reddy et al. 2017; Oliveros et al. 2019; Harvey et al. 2020; Stiller et al. 2024). Many relationships among birds are now strongly

corroborated across studies, providing a reliable framework for evaluating the accuracy of alternative approaches to estimate macrophylogenies. Another advantage of birds as a model system is the partial standardization of phylogenomic data collection through the widespread use of targeted enrichment of nuclear loci, such as ultraconserved elements (UCEs sensu Faircloth et al. 2012). Over a quarter of all avian species now have UCE data available (see below). These data have been used to resolve phylogenetic relationships among birds at both deep (e.g., McCormack et al. 2013; Jarvis et al. 2014; Oliveros et al. 2019; Harvey et al. 2020) and shallow (e.g., Smith et al. 2014; Winker et al. 2018) timescales. Most UCE studies of birds target a large, uniform set of loci (uce-5k-probe-set, available from https://github.com/faircloth-lab/uce-probe-sets; e.g., Sun et al. 2014). Some studies instead use a smaller, nested subset of these loci (uce-2.5k-probe-set) that is sometimes combined with exons commonly used in avian phylogenetics (e.g., Smith et al. 2014; Harvey et al. 2020). Although these datasets exhibit some heterogeneity – stemming from the use of different bait sets and variability in the quality of input DNA templates – extensive overlap facilitates integration into a single comprehensive dataset.

In this study, we use phylogenomic data from birds to empirically evaluate the accuracy and computational cost of alternative tree estimation approaches. By assembling orthologous UCE loci from the primary literature, we aim to better understand the factors influencing the estimation of macrophylogenies. Specifically, we address the following questions: 1) Do computationally efficient methods, such as "fast" maximum likelihood (ML) estimation, supertrees, or a divide-and-conquer strategy that combines many small trees using a supertree method, recover similar numbers of expected relationships corroborated in prior studies as traditional ML methods? 2) Does filtering datasets to reduce size and heterogeneity result in topologies that recover fewer expected clades, and how does it affect compute time? 3) Does the use of different methods, which may bias branch length estimation and produce distinct topologies, affect divergence time estimation? By combining phylogenomic data from independent studies, we constructed a large-scale avian phylogeny, encompassing 2,756 ingroup taxa, 2 outgroup taxa and 5,121 loci. Our findings demonstrate that it is possible to infer an accurate macrophylogeny with moderate computational cost. Moreover, the strategies

identified as most effective in this study are likely applicable to other taxonomic groups with sufficient phylogenomic data.

#### **Materials and Methods**

### Assembling the phylogenomic data

We took multiple approaches to create a database of UCE loci from existing studies of birds. We downloaded much of the data as individual alignments from 22 phylogenomic studies (Zhang et al. 2014; Bryson et al. 2016; Hosner et al. 2016; Manthey et al. 2016; McCormack et al. 2016; Burga et al. 2017; Campillo et al. 2018; Andermann et al. 2019; Andersen et al. 2019; Everson et al. 2019; McCullough et al. 2019a; McCullough et al. 2019b; Oliveros et al. 2019; Sackton et al. 2019; White and Braun 2019; Harvey et al. 2020; Imfeld et al. 2020; Oliveros et al. 2020; Salter et al. 2020; Smith et al. 2023; Braun et al. 2024; for details, see Supplementary Table S1 & Supplementary Information). We noticed that several studies had overlapping or nested taxon sampling. For example, Moyle et al. (2016) collected UCE data for 104 songbird species, and these data had all been included in a later study with broader taxon sampling (Oliveros et al., 2019). Therefore, we used the dataset from Oliveros et al. (2019) for downstream analyses.

All studies targeted UCEs as the main genetic markers (some also targeted a small number of legacy markers), and we preferentially downloaded alignments with as little filtering as possible (e.g., no missing data cut-offs). For studies where individual alignments were unavailable, we downloaded concatenated matrices and partition files, which we converted into alignments using the "split" function of AMAS (Borowiec 2016). Finally, we extracted UCEs and 500 bp flanking sequences from genome assemblies available at NCBI (that were not under embargo; data downloaded on October 14, 2020) for species that were not represented by UCE sequences, following Tutorial III of PHYLUCE (Faircloth 2016) with the 5k probe set.

We processed the sequences to retain only one individual per species, according to the IOC World Bird List v13.1 (Gill et al. 2023). When multiple individuals of the same species were present in our alignments or the same sample was used in different studies, we arbitrarily selected the representative sample based on the alphabetical order of the studies

(Supplementary Table S1). A few exceptions arose from taxonomic changes, occasionally causing minor duplication or inclusion of multiple subspecies representing the same species (see Data Availability). After verifying taxa, we performed sequence alignment with MAFFT (Katoh and Standley 2013) using default settings and the --adjustdirection option to correct for sequence orientation. Then, we filtered raw alignments with trimAl (Capella-Gutiérrez et al. 2009) using the "gappyout" method to remove sites based on the gap distribution within each alignment. We refer to these alignments as the "full" dataset. We anticipated substantial heterogeneity in the original datasets used to generate our supermatrix. See Supplementary Information for how we evaluated data heterogeneity.

### Filtering loci and subsetting datasets

185

186

187

188

189

190

191

192

193

194

195

196

197

198

199

200

201

202

203

204

205

206

207

208

209

210

211

212

213

To assess how different locus filtering schemes affect topology and computational cost, we created 27 filtered datasets by applying three filtering schemes serially to the full dataset (Fig. 1a). First, to control for missing sequence data by taxon, i.e., effects of partial sequences, or "type II" missing data (sensu Hosner et al. 2016), we prepared two datasets where we removed taxa from alignments when they were shorter than 50% or 75% of the longest sequence in the alignment for each locus (Fig. 1a, Step I). Then we ran these two datasets, plus the full dataset, through a second stage of filtering to control for gappyness by retaining alignment positions with at least 90%, 70%, and 50% occupancy (Fig. 1a, Step II). This step helps to address potential issues with indel-induced alignment gaps (e.g., Dwivedi and Gadagkar 2009) and reduce heterogeneity that can occur at the ends of UCE alignments. Finally, for each of the nine datasets that resulted, we performed a third stage of filtering to control for taxon completeness, where we retained loci with at least 90% (n = 2,484), 70% (n = 1,932), and 50% (n = 1,380) of the total number of taxa (Fig. 1a, Step III). The last step helps to control for the effects of incomplete taxon sampling, i.e., "type I" missing data (sensu Hosner et al. 2016). We concatenated each of these datasets using PHYLUCE (Faircloth 2016) prior to phylogenetic analysis.

For each filtered dataset and the full dataset, we averaged the individual-based summary statistics (see Supplementary Information) across all taxa sampled in that dataset (Supplementary Table S2). To visually inspect if taxa were clustering by study, we performed

principal component analysis (PCA) using FactoMineR v1.34 (Lê et al. 2008) on individual-based summary statistics and plotted the first two principal components using ggplot2 v3.3.5.9 (Wickham 2011) in R (R Core Team 2023). We also used IQ-TREE2 (Nguyen et al. 2015) to compute locus-based summary statistics for each filtered dataset, i.e., number of loci, total sites, parsimony informative sites, average gap and ambiguity across all loci, and loci with more than 50% missing data (Supplementary Table S3). We used ComplexHeatmap (Gu 2022) to plot the locus-based summary statistics for 27 filtered datasets (Fig. 1b).

### **Initial data exploration**

### - Concatenated analyses

We used the message passing interface (MPI) version of RAXML-NG v1.0.1 (Kozlov et al. 2019) to infer a ML phylogeny of the concatenated, full dataset (Table 1, baseline). Because this dataset was large, we ran two concurrent ML analyses that each used 800 CPUs – both used the GTR+R4 site rate substitution model, but one used parsimony to generate starting trees (MP starting trees) while the other used random starting trees. Because of the compute hours allocated to this project, we were only able to infer seven ML phylogenies using random starting trees and five ML phylogenies using MP starting trees for the RAXML-NG analysis. We selected the optimal tree as the one having the highest log-likelihood across the 12 analyses. We generated support values for the full dataset by performing ML analysis on 10 standard bootstrap (Felsenstein 1985) replicates with the GTR+R4 model. We evaluated the bootstrap replicates for convergence using the –bs-converge option. We found that these replicates had converged, and we reconciled the "best" ML tree with the bootstrap replicates using RAxML-NG.

To explore a faster method for ML tree estimation, we used the -fast option in IQ-TREE v2.0.5 (Nguyen et al. 2015) with the GTR+G site rate substitution model (Table 1, strategy 1). We initially inferred phylogenies from the concatenated, full dataset along with six filtered datasets that varied in numbers of loci, informative sites, and amounts of missing data. This "fasttree" approach resembles FastTree (Price et al. 2010), although it estimates two starting trees (using BIONJ (Gascuel 1997) and MP). It then optimizes the trees using rapid hill climbing

including stochastic nearest neighbor interchanges (NNI), and increased tolerance on likelihood values to speed up optimization, which has the potential to reduce accuracy (for detailed steps, see Supplementary Information).

Following the inference of trees from concatenated datasets, we performed an initial quality check of the inferred phylogenies by visual assessment of the relationships, and we pruned *Muscipipra vetula* and *Spheniscus mendiculus* from trees using the drop.tip function in ape v5.7-1 (Paradis and Schliep 2019) because these appeared in positions that were unlikely.

#### - Coalescent species tree estimation

242

243

244

245

246

247

248

249

250

251

252

253

254

255

256

257

258

259

260

261

262

263

264

265

266

267

268

269

For the full dataset and each of the six filtered datasets, we estimated individual gene trees using IQ-TREE v2.1.3 (Minh et al. 2020) under the GTR+G model, and we combined the ML trees to generate a species tree using ASTRAL v5.7.8 (Zhang et al. 2018) (Table 1, strategy 2).

### - Building supertrees using existing phylogenomic trees

Supertree methods (Table 1, strategy 3) infer phylogenies from existing trees, and we identified 53 trees from 46 phylogenomic studies (McCormack et al. 2013; Jarvis et al. 2014; Lamichhaney et al. 2015; Nater et al. 2015; Prum et al. 2015; Bryson et al. 2016; Hosner et al. 2016; Manthey et al. 2016; Ottenburghs et al. 2016; Zarza et al. 2016; Burga et al. 2017; Reddy et al. 2017; Wang et al. 2017; White et al. 2017; Yonezawa et al. 2017; Andersen et al. 2018; Bruxaux et al. 2018; Campillo et al. 2018; Chen et al. 2018; Ferreira et al. 2018; Musher and Cracraft 2018; Younger et al. 2018; Andermann et al. 2019; Andersen et al. 2019; Everson et al. 2019; McCullough et al. 2019a; McCullough et al. 2019b; Oliveros et al. 2019; Sackton et al. 2019; White and Braun 2019; Harvey et al. 2020; Imfeld et al. 2020; Oliveros et al. 2020; Salter et al. 2020; Smith et al. 2020; Vianna et al. 2020; Catanach et al. 2021; Kirchman et al. 2021; Oliveros et al. 2021; McCullough et al. 2022; Vinay et al. 2022; Wang et al. 2022; Smith et al. 2023; Zhao et al. 2023; Braun et al. 2024; for details, see Supplementary Table S4) which have overlapping taxa with those included in the supermatrix datasets. After obtaining tree files representing all studies (see Supplementary Information), we reconciled the taxon names to match those in IOC v13.1 and pruned duplicate tips that represented the same species within a tree using the drop, tip function in ape.

Because the phylogenomic trees we downloaded included few taxa that overlapped among studies, we integrated them using three types of backbone trees: one from Burleigh et al. (2015) that we refer to as the "Burleigh backbone", a second from Jetz et al. (2012) that we refer to as the "Jetz backbone", and a "taxonomic" backbone (family-level or genus-level). See Supplementary Information for how we generated the Burleigh and Jetz backbones. We created the family-level taxonomic backbone based on taxon names in IOC v13.1 to: group individual taxa by family, cluster taxa from same family into a polytomy, cluster families from the same order into a polytomy, and cluster orders into infraclasses Palaeognathae,

Galloanserae, and Neoaves. Finally, we enforced a tree topology to reflect a well-established topology: (outgroup,(Palaeognathae,(Galloanserae,Neoaves))). We constructed the genus-level taxonomic backbone similarly by clustering taxa from the same genus into a polytomy, then clustering by family, order, and infraclass and enforcing the same topology among infraclasses.

We used matrix representation with parsimony (MRP) (Baum 1992; Ragan 1992) to generate supertrees following the pipeline described in Kimball et al. (2019). Since the supertree method can suffer from source tree incongruence (Bininda-Emonds et al. 2002), we employed a user-guided weighting scheme to address topological conflicts among source trees. Specifically, we assigned different weights to input trees based on the amount of data used to infer them (Supplementary Table S4) by including from one (low weight) to eight (high weight) copies in the supertree matrix. For example, trees based on whole-genome sequencing data, such as the Jarvis TENT tree (Jarvis et al. 2014), were given a weight of eight and included in the supertree matrix eight times. We typically weighted UCE trees as four. However, if a study included two UCE trees estimated by different approaches (e.g., methods of tree estimation or filtering strategies) but using completely or largely overlapping data, we assigned each tree a weight of two. We assigned two additional trees (Reddy et al. 2017; Yonezawa et al. 2017) a weight of two because they were based on a large number of "legacy markers" (Kimball et al. 2009) extracted from genome assemblies. Finally, we assigned a weight of one to all backbone trees.

After determining the weighting scheme, we created three supertree matrices: 1) weighted trees with the Burleigh and Jetz backbones; 2) weighted trees with Burleigh, Jetz, and

family-level taxonomic backbones; and 3) weighted trees with Burleigh, Jetz, and genus-level taxonomic backbones. Then we used CLANN (Creevey and McInerney 2005) to convert the input tree matrix to a binary (MRP) representation and generated supertrees using PAUP\* v4.0 (Swofford 2003). We conducted the searches using the parsimony ratchet (Nixon 1999) as described in Kimball et al. (2019), which used code available from https://github.com/ebraun68/ratchblock to generate PAUP blocks that ran five tree searches with different upweighting scores. Each tree search consisted of 100 replicates and produced a strict consensus tree from these replicates after the tree search concluded. For each of the three matrices, we selected the resulting supertree as the one from the five searches that had the best parsimony score. Then we pruned the resulting three supertrees to include only the taxa present in the full (supermatrix) dataset, which resulted in 2,751 taxa (seven taxa in our supermatrix were not included in published phylogenies).

#### - Building supertrees using a divide-and-conquer approach

Because supermatrix methods can be computationally intensive for large datasets, we also tested a divide-and-conquer approach that combined supermatrix and supertree methods by dividing the supermatrix into subsets of taxa, inferring trees from each subset using supermatrix methods, then integrating the resulting subset trees with supertree methods (Table 1, strategy 4). To begin the process, we designed three subsetting schemes that differed in the likely number of overlapping taxa shared between them: random subsets, partially stratified subsets, and fully stratified subsets.

We created 15 random subsets by randomly drawing (with replacement) 150 taxa from the total list of taxa (2,760) in the full dataset.

We created the partially stratified subsets by dividing all taxa in the full dataset into six major groups that were recovered across many studies (Supplementary Figure S1). Then, we randomly selected 7.5%, 3.1%, 7.8%, 6.8%, 7.4%, and 8.0% of the taxa within each group largely based on its size while avoiding oversampling suboscines, which produced a subset of 150 taxa. We repeated this selection process without replacement to create a total of 10 partially stratified subsets.

We created the fully stratified subsets by dividing all taxa in the full dataset into 25 groups (Supplementary Figure S2) that were based on taxonomy to ensure all taxa were represented at least once across the subsets and were included in trees with congeners (so sister relationships could hopefully be resolved). We set the number of taxa included in each subset under 200 to maximize computational efficiency given our resources (see Supplementary information). Because supertree analyses require overlapping taxa, we then manually selected "linker taxa" from outside each group and included them in the group membership. Preliminary analyses showed that using identical linker taxa across fully stratified subsets placed the linker taxa in unexpected positions in the resulting tree. Therefore, we used distinct linker taxa for each subset, which resolved this issue.

We created a total of 50 subsets across all schemes. We extracted subset alignments from the aligned, concatenated, full dataset. Then, we used IQ-TREE v2.1.3 (Minh et al. 2020) to infer the "best" ML phylogenies and generate 1,000 ultrafast bootstrap replicates for each subset using the GTR+R4 model.

We followed the same weighted-tree search approach described above to infer a set of supertrees representing all taxa from the 50 "best" ML subtrees. Specifically, we created five supertree matrices using: 1) the 50 best ML subtrees where each tree was given a weight (w) of one (w = 1); 2) the 50 best ML subtrees (w = 4) and the family-level backbone tree (w = 1); 3) the 50 best ML subtrees (w = 2) and the family-level backbone tree (w = 1); 4) the 50 best ML subtrees (w = 4) and the genus-level backbone tree (w = 1); and 5) the 50 best ML subtrees (w = 2) and the genus-level backbone tree (w = 1).

We also built 1,000 MRP matrices (each with 50 trees) from the bootstrap replicates by sampling and combining replicates from the subsets in the order they were generated: bootstrap replicate tree one from all 50 subsets combined to form MRP matrix one, bootstrap replicate tree two from all 50 subsets combined to form MRP matrix two, et cetera. Then we performed the tree search process described above for each MRP matrix to produce a set of 1,000 phylogenomic supertrees that we summarized to a 50% majority rule consensus using SumTrees (Sukumaran and Holder 2010). We pruned the six supertrees generated from the steps above to include only the taxa present in the full (supermatrix) dataset.

### **Analyzing tree distances**

356

357

358

359

360

361

362

363

364

365

366

367

368

369

370

371

372

373

374

375

376

377

378

379

380

381

382

383

To visually represent differences between the various trees we inferred, we rooted trees on the crocodilian outgroup and used ete3 (Huerta-Cepas et al. 2016) to calculate pairwise normalized Robinson-Foulds distances between the two trees inferred from the full dataset, the six trees inferred from the filtered datasets, the three trees inferred from the supertree analyses, and the six trees inferred using the divide-and-conquer approach (Table 1). ASTRAL species trees were not included (see Results). We used the write nexus dist function in phangorn v2.11.1 (Schliep 2011) to create a NEXUS block of the pairwise Robinson-Foulds distances, and we used PAUP\* v4.0 (Swofford 2003) to infer a neighbor-joining (NJ) "tree-of-trees" that we rooted at the midpoint.

### **Testing for clade monophyly**

Sangster et al. (2022) and earlier work (Chen and Field 2020; Queiroz et al. 2020; Sangster and Mayr 2021) highlighted several clades near the base of the avian tree that are very likely to reflect the true species tree. Modern taxonomies, such as IOC, eBird/Clements (Clements et al. 2023), and Howard & Moore (Dickinson and Christidis 2014), now circumscribe orders, families, and genera in ways that largely align with recent phylogenetic insights. However, no current taxonomy is without limitations. Some families and genera continue to be refined as more information becomes available. Although there are almost certainly some named taxa that do not represent clades in the true species tree, the majority of named groups are likely to be expected clades. We compared how reliably the different tree inference methods resolved these expected clades across the avian phylogeny. These include orders, families, and genera recognized by IOC v13.1, as well as 33 high-level clades (e.g., superorder, infraclass). We generally assumed that a method was more reliable when it recovered a larger number of these groups as monophyletic (e.g., Portik and Wiens 2021). To perform these analyses, we first excluded clades that were only represented by a single species. Then we used the AssessMonophyly function in MonoPhy (Schwery and O'Meara 2016) to calculate how many of the 410 evaluated genera, 138 evaluated families, 40 evaluated orders, and 33 evaluated highlevel clades were not resolved as monophyletic.

#### **Summarizing compute time**

384

385

386

387

388

389

390

391

392

393

394

395

396

397

398

399

400

401

402

403

404

405

406

407

408

409

410

411

412

We summarized and compared the compute time required for the tree inferences described above. To increase our computational capacity, analyses were run across several different computing systems: HPC@LSU (RAxML-NG analysis; https://www.hpc.lsu.edu/), AMNH Huxley HPC (initial fasttree analyses and ASTRAL analyses; https://www.amnh.org/research/computational-sciences), and UF HiPerGator (supertree and divide-and-conquer analyses; https://www.rc.ufl.edu/about/hipergator/). For each analysis, we tallied the CPU hours spent for tree searches (including bootstrap replicate searches if applicable) and optimization, and we collected the total cluster utilization for each SLURM job. For the RAxML-NG analysis of the full dataset, we combined the CPU time for the random and the MP starting trees. For the divide-and-conquer analyses, we summed the CPU hours spent for tree search across 50 subsets. Because the supertree component for the divide-and-conquer analyses used very little CPU time compared to the subset concatenation analysis, we added it directly to the total CPU time spent (for the bootstrap trees, time for 1,000 runs were added). For the regular supertree analyses, we presented the PAUP tree search time and added time for MRP matrix construction to the total CPU hours spent. To account for variations in CPU hardware performance across the three computing systems, we used the base and turbo clock speed to calculate the theoretical minimum and maximum giga floating-point operations per second (GFLOPS; 1 GFLOPS = 10<sup>9</sup> FLOPS) per core (Supplementary Table S5). This metric was then used to evaluate the relative performance of each computing system and to adjust the CPU cost accordingly (adjusted CPU time = CPU hours \* GFLOPS).

### Tests on two filtered datasets

Generating the distance matrix and BIONJ starting tree in the initial fasttree analyses was time-consuming for our datasets. However, the likelihood of the resulting fasttree was only slightly improved compared to the MP starting tree, and the MP starting tree was always much better than the BIONJ tree (Supplementary Table S6). To improve fasttree search and optimization, we examined the role of the starting tree using two filtered datasets (filter1 and filter3). We chose these filter sets due to their contrasting patterns of expected clade recovery in initial exploration: filter1 performed well deeper in the tree but poorly at the tips, whereas filter3

showed the opposite pattern. Fasttree searches normally use two starting trees (MP and BIONJ), however, users can supply their own starting tree to bypass the default starting tree estimation process. We performed a total of 24 additional tree searches for each dataset with different starting trees (see Supplementary Information). We evaluated the log likelihoods of the starting tree and optimal tree and assessed expected clade recovery for the final ML tree in each analysis (Supplementary Table S7).

Based on the tests using filter1 and filter3, we found that searches initiated with BIONJ and MP starting trees required a large amount of time, had a much lower likelihood, and resulted in worse expected clade recovery than the initial exploration (Supplementary Figure S3 and Supplementary Table S7). In contrast, fasttrees built using only MP starting trees derived from the same filtered dataset used for the ML search consistently had much better likelihoods than those derived from other filtered datasets. These results suggest a straightforward method to improve the speed and reproducibility of fasttree searches: avoid generating the BIONJ tree and instead conduct multiple searches using MP starting trees generated from the same dataset used for the fasttree search.

#### New fasttree method with MP starting trees

We used Parsimonator v1.0.2 (https://github.com/stamatak/Parsimonator-1.0.2) to estimate four MP starting trees (parsA, parsB, parsC, and parsD; different random number seeds for each search) for each of the full and 27 filtered datasets. Each MP starting tree was used to run a fasttree analysis in IQ-TREE v2.2.2 (Nguyen et al. 2015) with parsA and parsB using the GTR+G model and parsC and parsD using the FreeRates model (GTR+R4). Two filtered datasets were identical to each other (indv75\_sites50\_loci90 and indv75\_sites70\_loci90), therefore we performed only one set of analyses for these two datasets. This resulted in a total of 108 new fasttrees, four for each dataset (Table 2). We evaluated their performance in expected clade recovery and summarized the total CPU time spent. We z-transformed each locus-based summary statistic across all filtered datasets and plotted using ComplexHeatmap with hierarchical clustering (Supplementary Figure S4). From each cluster, we selected a representative dataset that performed best in recovering expected clades. We only present the

best fasttree for these representative datasets in the main text (see complete results in Supplementary Table S8).

### **Hybrid approaches**

We tested whether fasttrees could improve the supertree and divide-and-conquer methods when used as backbone trees. Unlike the Jetz+Burleigh backbones used initially, our fasttrees included all taxa in the analyses, potentially providing a better backbone to compensate for limited overlap among source trees. Additionally, because our fasttrees were estimated from phylogenomic data, they may offer a more accurate representation of relationships, potentially reducing the need for taxonomic backbones. We referred to these new approaches as the "hybrid supertree approach" and "hybrid divide-and-conquer approach" (Table 2).

We used the two best new fasttrees (based on expected clade recovery) and seven initial fasttrees as the backbone tree in supertree and divide-and-conquer analyses (Table 2). For the hybrid supertree approach, we conducted two sets of nine analyses (with or without a family-level taxonomic backbone), each analysis with a different fasttree as the backbone. Each backbone was given a weight of one, and source trees were given different weights based on the amount of data used to infer them, as described above. For the hybrid divide-and-conquer approach, we also ran two sets of analyses, each with nine trees estimated: 1) using only a fasttree as the backbone with the 50 best ML subtrees and the fasttree backbone each given a weight of one; and 2) using a fasttree backbone and a genus-level backbone with the 50 best ML subtrees given a weight of one. We then followed the same steps described above to build a binary MRP tree matrix in CLANN and generate supertrees using PAUP\*. Similarly, we evaluated the performance in expected clade recovery for final output trees (Supplementary Table S9). When summarizing the total CPU time spent, we added in the compute time for generating each MP starting tree and the fasttree. All new fasttrees, MP starting trees, and hybrid approaches were run on UF HiPerGator HPC.

### Molecular dating

We applied a total of 43 fossil calibrations for node-dating analyses (Supplementary Table S10) following best practices proposed by Parham et al. (2012), and we assigned minimum and

maximum possible ages to each calibrated node in our phylogeny. Additional information regarding the fossils selected to calibrate divergence time analyses is presented in the Supplementary Information.

Then, due to the size of the resulting trees, we used TreePL (Smith and O'Meara 2012) to estimate divergence times for the (1) RAxML-NG tree inferred from the concatenated, full dataset; (2) two fasttrees using new fasttree methods based on the full dataset and the filtered dataset indiv0\_sites50\_loci50; 3) two supertrees (one from initial exploration and one from the hybrid approach); and 4) two divide-and-conquer trees (one from initial exploration and one from the hybrid approach). For the four supertrees and divide-and-conquer trees, we used IQ-TREE2 v.2.2.2 (Nguyen et al. 2015) to optimize the tree branch lengths (--tree-fix) under both GTR+G and GTR+R4 model using the filtered dataset with the smallest amount of missing data (indv0\_sites90\_loci90). TreePL allows for varying rates across branches but penalizes rate differences over the tree with a rate smoothing parameter, so we identified the optimal rate smoothing parameter through cross-validation that tested 10 values (start = 1e-07; stop = 10,000). We also used the "prime" option to identify the best optimization parameters and the "thorough" option to allow the program to iterate until convergence.

We extracted crown ages only for groups that were monophyletic across seven time trees and compared the age of each group across trees. We also compared the time estimates for 12 major groups (that have been consistently resolved across studies and that represent both ancient and recently diverged clades as well as both fast- and slow-evolving clades) to those in other studies (Claramunt and Cracraft 2015; Prum et al. 2015; Kimball et al. 2019; Kuhl et al. 2021; Brocklehurst and Field 2024; Claramunt et al. 2024; Stiller et al. 2024; Wu et al. 2024a). Divergences estimated under GTR+G and GTR+R4 models were very similar (see Data Availability), thus only results from GTR+R4 model were used for presentation. We also computed relative divergence time for these clades by scaling the divergences to Neognathae.

### Results

Taxon sampling

Our UCE data matrix contained DNA sequence alignments for 5,121 target captured loci, with an average length of 665 base pairs (bp) and a total of 2,047,980 parsimony informative sites. The full dataset contained 2,758 tips (including two crocodilian outgroups); members of all 44 extant bird orders and one extinct order (Dinornithiformes); 250 of 253 (98.8%) extant bird families and one extinct family (Emeidae); 1,081 genera; and 2,747 unique species.

### **Dataset characteristics and filtering**

Data heterogeneity was evident in descriptive statistics for individual taxa. For instance, taxa showed considerable variation in locus count, sequence length, and individual-based parsimony informative sites both within and between studies (Supplementary Figure S5). PCA of these summary statistics revealed distinct clusters corresponding to their source datasets (Supplementary Figure S6). As anticipated, more stringent filtering schemes substantially increased homogeneity among studies and reduced the amount of missing data. However, these improvements reduced the number of informative sites (Supplementary Figure S5).

#### Baseline phylogeny

The RAxML-NG tree of the full concatenated dataset recovered all 33 high-level clades identified by Sangster et al. (2022), all 40 evaluated orders (excluding monotypic or single-sampled orders), all but two of the 138 evaluated families, and all but 38 of the 410 evaluated genera (Fig. 2; Supplementary Figure S7).

Although the RAxML-NG tree appeared to provide an accurate estimate of avian phylogeny based on expected clade recovery, generating this tree required significant computational resources – approximately 428,000 CPU hours for the primary search and additional 323,000 CPU hours for a limited number of bootstrap analyses.

# **Initial exploration**

We explored four alternative approaches (Table 1) that were more computationally efficient than standard ML: (1) implementing a fast ML estimation approach, (2) estimating individual

gene trees and combining them into a species tree, (3) combining source trees into a supertree, and (4) using a divide-and-conquer strategy in which trees were estimated from data subsets and then combined into a supertree. The primary goal of these analyses was to determine whether any of these computationally efficient methods could produce trees as accurate as the RAxML-NG tree.

The fasttree (Table 1, strategy 1) estimated from the full dataset did not perform as well as either the RAxML-NG tree or the best trees from other approaches (Fig. 3). Filtering appeared to improve the performance of fasttree analyses, with the best results based on the expected clade recovery criterion observed in trees inferred from the least aggressively filtered datasets (filter1 and filter2). By contrast, the most aggressively filtered datasets (filter5 and filter6) performed poorly with clade recovery similar to that of the full dataset fasttree, suggesting diminishing returns with overly stringent filtering.

The ASTRAL species trees (Table 1, strategy 2) recovered substantially fewer expected clades than either the RAxML-NG tree or the fasttrees, regardless of the filtering procedure (or lack thereof) used to generate the alignments for gene tree estimation. The total number of unresolved groups ranged from 144 to 207 and adjusted CPU time (CPU hours \* GFLOPS) ranged from 29,549 to 1,977,494 (Supplementary Table S11).

For the supertree analysis (Table 1; strategy 3), the supertree constructed without taxonomic backbones (S1) performed poorly in recovering expected clades (Fig. 3). In contrast, the two supertrees with taxonomic backbones (S2 & S3) performed as well as, or slightly better than, the RAxML-NG tree in terms of expected clade recovery while still requiring minimal compute time (Fig. 3).

The divide-and-conquer approach (Table 1, strategy 4) without taxonomic backbones outperformed the supertree without backbones in recovering expected clades (Fig. 3). However, performance comparable to the RAxML-NG tree was achieved only when a genus backbone was included. Despite requiring the estimation of input trees from the supermatrix, this method was much more computationally efficient than the RAxML-NG analysis (Fig. 3).

The two divide-and-conquer trees using the genus backbone (T5 & T6) performed well overall but exhibited polytomies within heavily sampled passerine families, such as Tyrannidae

and Thamnophilidae, as well as among some oscine families. Notably, these polytomies were not observed in Oliveros et al. (2019) and Harvey et al. (2020), which were the sources of most of the passerine data. The number of polytomies decreased when the weight of the source trees relative to the genus backbone was reduced (lower in T6 [2:1] versus higher in T5 [4:1]; see Supplementary Information for details on comparing polytomies). However, this adjustment did not affect the recovery of expected clades.

The tree-of-trees (Fig. 3) indicated that the method of inference (supermatrix, supertree, or divide-and-conquer) strongly influenced topological similarity. Notably, supertree and divide-and-conquer methods formed distinct clusters. For the supertrees, this clustering may reflect biases introduced by relationships within the source trees, which differed from those inferred using other methods. Similarly, the clustering of divide-and-conquer analyses likely stems from the use of the same underlying subset trees (or their bootstrap consensus), which may have contributed unique relationships within the data subsets. By contrast, the fasttrees did not form a single cluster, and branch lengths in the NJ tree indicated greater variation among these analyses compared to the other methods. This increased variation is expected, given that the fasttree datasets differed in content due to filtering.

#### **Fasttrees with MP starting trees**

We conducted four searches on the full dataset and each of the 27 filtered datasets. Analysis of expected clade recovery for all new fasttrees (Supplementary Table S8) revealed that one fasttree from the full dataset (using an MP starting tree with the GTR+R4 model in replicate search D, i.e., FreeRates parsD) matched the RAxML-NG tree in both the number and identity of expected clades (Figs. 4 & 5). This best full dataset fasttree closely approximated the RAxML-NG tree in tree space (Fig. 4), but it was far more computationally efficient (69- to 178-fold difference in the adjusted CPU costs between the two analyses, depending on the dynamic CPU speed).

We compared the performance of filtered datasets to evaluate the effects of different filtering strategies. At the genus level, datasets filtered with indv0 and loci50 (keeping all taxa within specific loci and retaining loci sampled in ≥50% of taxa) achieved the best expected clade recovery. For high-level clades, datasets filtered with sites50 (removing alignment columns

where  $\geq$ 50% of taxa were gaps or missing) performed best. In contrast, more aggressive filtering approaches, such as loci90 (retaining loci sampled in  $\geq$ 90% of taxa) and indv75 (keeping taxa with  $\geq$ 75% of sequence completeness), consistently resulted in poorer clade recovery. As expected, filtering reduced the number of sites and CPU time was positively correlated with the size of the supermatrix across all fasttree analyses (R<sup>2</sup> = 0.8; Supplementary Figure S8). While we observed no consistent pattern in clade recovery between trees estimated with FreeRates and GAMMA models, GAMMA models generally required less compute time.

### Hybrid supertrees and hybrid divide-and-conquer trees

Using a fasttree backbone in the hybrid supertree approach led to poor clade recovery, with some iterations performing worse than our initial analyses using the Jetz+Burleigh backbones (Fig. 4 and Supplementary Table S9). However, as in the initial analyses, adding a taxonomic backbone greatly improved performance, with several hybrid supertree analyses recovering more expected clades than the RAxML-NG tree. Despite these improvements, a better backbone did not eliminate the novel relationships introduced in the supertree analyses. Hybrid supertrees still produced topologies that were the most divergent from those inferred by RAxML-NG, our best new fasttrees, or our best hybrid divide-and-conquer trees (Fig. 4).

The hybrid divide-and-conquer trees were similar to the RAxML-NG tree (Fig. 4). However, even when using a fasttree with strong expected taxa recovery (e.g., the fasttree fulldata parsD), these trees recovered fewer expected clades than the RAxML-NG analysis. While the inclusion of a taxonomic backbone provided some improvement, none of the hybrid divide-and-conquer trees outperformed the best hybrid supertrees (Fig. 4). Additionally, some polytomies observed in the initial analyses persisted, even with the inclusion of both the fasttree and a taxonomic backbone.

### **Divergence time estimation**

Divergence time estimates for key nodes were generally similar across our seven trees (Fig. 7), despite being estimated using different methods and datasets. Lower-level ranks, e.g., genus, in general showed higher variation in crown ages across trees when compared to higher-level ranks (Fig. 7a). However, the number of outliers (points that fell outside 1.5x the interquartile

range for all clades of the same rank) was smaller as a proportion of the total clades considered in lower-level ranks. Recent studies also show broadly similar relative divergence times (to Neognathae) for comparable groups (Fig. 7b), although there were differences among time trees (especially for published studies) in the absolute divergence times (Fig. 7c).

612

613

614

615

616

617

618

619

620

621

622

623

624

625

626

627

628

629

630

631

632

633

634

608

609

610

611

### Discussion

### Baseline phylogeny and expected clade recovery

The RAxML-NG tree provided a reliable estimate of the bird phylogeny, and most cases of non monophyly at lower taxonomic levels matched results from recently published phylogenomic studies (e.g., Harvey et al. 2020; Smith et al. 2023). Some instances of non-monophyly likely reflected artifacts, such as limited taxon sampling or insufficient sequence data, particularly from historical museum specimens, while others appear to reflect the true phylogenetic relationships of genera or families for which formal taxonomic revision is pending (e.g., Tyranneutes nested in Neopelma (Leite et al. 2021), Antilophia in Chiroxiphia (Zhao et al. 2023), and Tityridae divided into Tityridae sensu stricto, Onychorhynchidae, and Oxyruncidae (Oliveros et al. 2019)). However, the RAxML-NG analysis required substantial computational resources, which was expected given the long-recognized challenges of large tree searches under the likelihood criterion (reviewed by Yang and Rannala 2012). The recently introduced Early Stopping version of RAxML-NG, which offers up to a 5-fold speedup for large DNA datasets and up to 10-fold speedup when using MP starting trees (Togkousidis et al. 2025), may reduce some of these computational demands. Conversely, incorporating MP starting trees to fasttree approaches significantly reduces the computational burden while producing trees that appear to be of approximately equal quality – providing a promising alternative for scaling future phylogenetic inferences including thousands of loci to even larger numbers of tips (5,000+).

### **Fasttree approaches**

As noted above, we evaluated alternative analytical approaches that might offer similar or even greater accuracy while requiring fewer computational resources than RAxML-NG. Our initial

exploration of computationally efficient methods found that fasttrees, while not as accurate as the RAxML-NG tree or the best-performing supertrees and divide-and-conquer trees, still demonstrated relatively good recovery of expected clades (Fig. 3). Previous studies found that trimming the alignments did not improve expected clade recovery (Tan et al. 2015; Portik and Wiens 2021). However, this was not the case for our initial fasttree analyses, since the fasttree based on the full dataset exhibited poorer clade recovery than most of the filtered datasets. This result suggests that the heterogeneity of the full dataset may interfere with fasttree searches, unlike the RAxML-NG analysis, which appeared more robust to heterogeneity.

We improved the fasttree search and optimization process by conducting four replicate searches, each initiated using an MP starting tree. This modification resulted in a best full dataset fasttree that achieved phylogenetic accuracy comparable to the RAxML-NG tree, yet with a substantially reduced computational burden (Fig. 4). Although the two trees differed in the arrangement of Otidimorphae, Columbimorphae, and Opisthocomiformes (Supplementary Figure S9), the relationships among high-level clades at the base of Neoaves remain a particularly challenging phylogenetic problem (reviewed by Braun et al. 2019), with no consensus achieved to date (cf. Stiller et al. 2024; Wu et al. 2024a).

In contrast to our attempts to improve search efficiency, dataset filtering approaches yielded mixed results. Unlike our initial analyses, filtering to remove missing data did not enhance new fasttree performance in recovering expected clades, likely because filtered datasets also had fewer parsimony informative sites (Fig. 6). This result agrees with the findings in Tan et al. (2015) and Portik and Wiens (2021) that filtering did not increase expected clades recovery. Additionally, we found that site filtering had a greater impact on high-level clade recovery, whereas locus and individual filtering more strongly influenced resolution of expected genera. The most effective filtering strategy likely depends on the taxonomic level of interest, and a significant benefit of the new fasttree approach is that testing various filtering strategies and models is more feasible due to the significantly reduced compute time. This efficiency also makes it possible to incorporate multiple replicates of tree search to account for stochasticity. As phylogenomic datasets continue to grow in size, further advancements in computational efficiency for tree estimation will remain essential.

#### Species tree methods on heterogeneous datasets

Results from the ASTRAL analyses are consistent with previous studies, which have shown that poor sequence recovery and missing data can bias gene tree summary methods (Liu et al. 2010; Springer and Gatesy 2014; Hosner et al. 2016; Xi et al. 2016; Zhao et al. 2025). One contributing factor is the distribution of informative sites in UCE alignments, which are disproportionately located near the ends of the alignments (Faircloth et al. 2012). These regions may be underrepresented when sequence recovery is poor, particularly in lower-quality samples such as those derived from historical museum specimens. Consequently, taxa with poor sequence recovery may be misplaced in estimated gene trees or excluded from certain gene trees altogether, leading to inaccuracies in the ASTRAL tree. Improving ASTRAL trees would entail excluding lower-quality samples and result in a tree with many fewer tips. Overall, ASTRAL was not an accurate method for estimating macrophylogeny with this type of heterogeneous UCE data, even when using the more homogenous filtered subsets. Additionally, ASTRAL was less computationally efficient than many of the other methods tested (Supplementary Table S11).

### Supertree and divide-and-conquer approaches

Despite being computationally efficient, the supertrees contained novel nodes that contradicted all input trees, potentially due to issues of hidden support (e.g., Gatesy et al. 2004; Wilkinson et al. 2005). While signals from the input phylogenomic trees should dominate the supertree topology due to their higher weights relative to the backbones, novel relationships likely arose from topological incompatibilities or asymmetric taxon sampling in the published phylogenomic trees used as input. These issues appeared to be intrinsic to the structures of the input trees (see examples in Supplementary Information). Consequently, hybrid supertrees still produced topologies that were the most divergent from other trees (Fig. 4). This outcome may be explained by the reliance of supertree methods on input trees generated using different analytical approaches by different investigators, as we combined trees from 46 distinct phylogenomic studies. Although the compute time required for supertree analyses was minimal (Fig. 3), this does not include the time needed to locate and code the source trees for analysis.

Overall, we were able to produce supertrees that provided reasonably accurate representations of the Avian Tree of Life, but the methods were not straightforward. Consistent

with previous studies, we found that incorporating backbones was critical for improving taxonomic overlap (Redelings and Holder 2017; Kimball et al. 2019; McTavish et al. 2024). An alternative or complementary approach involves pruning problematic taxa from the source trees (Bininda-Emonds et al. 2002) or upweighting more accurate source trees (Bininda-Emonds and Sanderson 2001). While these strategies can improve phylogenetic accuracy, they require prior knowledge and subjective decisions about phylogenetic relationships, which may not always be feasible or unbiased.

Compared to typical supertree approaches, the divide-and-conquer method has advantages, as the individual trees integrated using supertree techniques are generated under consistent programs, parameter settings, and computing platforms. This approach establishes a direct link between sequence data and supertree estimation, addressing the data-dissociation problem inherent in traditional supertree methods (e.g., Moore et al. 2006). However, all our divide-and-conquer trees, even with the taxonomic backbones, included unresolved nodes which were particularly evident in species-rich clades where limited overlap in taxon sampling across subsets may have contributed to the increased number of polytomies. This suggests that the 50 subsets used for the divide-and-conquer analyses were insufficient and that additional subsets may be required to improve resolution, albeit at the cost of increased compute time.

Although the source trees differed between the supertree and divide-and-conquer analyses, both used the same approach to estimate the final tree and faced similar limitations. In both cases, the best results were achieved using taxonomic backbones. While standardized taxonomic backbones are available for well-studied groups like birds, their absence in many other taxonomic groups limits the broader applicability of these methods. Even where these backbones are available, vastly different ranks may be used for clades of similar ages and species numbers in different parts of the Tree of Life. For example, there are 14,348 named ant species (Bolton 2025) and the ant crown group has an age of approximately 127 Ma (Borowiec et al. 2025), making the ants slightly more species-rich and older than birds. However, ants are classified as a family (Formicidae), rather than a class like birds, and this limits the number of taxonomic ranks that can be used for a supertree backbone or in assessment of clade recovery. Overall, these issues may limit the utility of supertree methods.

Identifying an appropriate weighting scheme for supertree methods is another challenge. The approach we used for our MRP gave a low weight for the backbone and assigned the largest weights to source trees based on the largest datasets, but it was ultimately ad hoc. Fortunately, the computational efficiency of supertree analyses allows for testing alternative weighting schemes (e.g., Moore et al. 2006; Baker et al. 2009; Nyakatura and Bininda-Emonds 2012) to evaluate their impact on resolution – provided robust criteria, such as expected clade recovery, are available for comparison. Finally, neither method inherently supports branch length estimation. Various approaches can assign branch lengths to supertrees, with or without molecular data (e.g., Purvis 1995; Bininda-Emonds et al. 1999; Torices 2010; Kimball et al. 2019). In our study, branch length-optimized supertrees and divide-and-conquer trees yielded divergence time estimates that were similar to those from the concatenated trees, suggesting this limitation may not be critical for most studies.

### Divergence time estimation

The timing of events in the avian phylogeny has been a topic of substantial debate. Some studies support an upper Cretaceous ancient origin for most high-level clades in Neoaves (Pacheco et al. 2011; Mitchell et al. 2015; Wu et al. 2024a; Wu et al. 2024b), while others suggest these lineages originated much closer to the Cretaceous-Paleogene (K-Pg) mass extinction event (~66 Ma) (Jarvis et al. 2014; Claramunt and Cracraft 2015; Prum et al. 2015; Kimball et al. 2019; Brocklehurst and Field 2024; Claramunt et al. 2024; Stiller et al. 2024). Despite these differences, all studies agree that crown birds originated in the mid- to late-Cretaceous, consistent with crown bird fossils predating the K-Pg boundary (e.g., Field et al. 2020).

Despite variation in tree topologies and branch lengths due to differences in data completeness, divergence time estimates were largely consistent across our methods (Fig. 7). This consistency held regardless of whether branch lengths were estimated during the tree search (RAxML-NG and fasttrees) or added later for methods that do not estimate meaningful branch lengths (supertree and divide-and-conquer analyses). These findings suggest that for downstream comparative analyses requiring time-calibrated trees, the choice of tree estimation method may have minimal impact, especially for deeper nodes, provided the

method reliably recovers topological relationships. These results, supported by our calibrations, corroborate the hypothesis that the rapid diversification of modern birds occurred near the K-Pg event. Taking these factors into account, we present the first "macrophylogenomic tree" for birds, a resource that can be leveraged in future comparative research.

### **Conclusions**

Overall, our analyses demonstrate that accurate macrophylogenies can be estimated using computationally efficient methods. This was achieved with a heterogeneous dataset assembled from many independent studies, reflecting the likely approach for estimating most large-scale phylogenies across the Tree of Life. While assembling such datasets introduces heterogeneity, our results demonstrate that filtering may not always be necessary. In fact, filtering can lead to lower accuracy, as we observed, where fewer expected clades were recovered from filtered datasets compared to the full dataset.

Our study employed the avian taxonomy from IOC v13.1 (2023) as the basis for the expected clades and the taxonomic backbones. This version provided a consistent and well-supported framework at the time of analysis. As ongoing research continues to refine our understanding of avian phylogenetics, more recent taxonomies can help resolve previously uncertain relationships. These updated resources can offer an even greater foundation for future studies, and our approach demonstrates the utility of a stable baseline for evaluating methodological performance.

Although we successfully estimated trees using several approaches that appeared accurate based on expected clade criterion, traditional supertree and divide-and-conquer methods required additional information, such as taxonomic backbones, to achieve results comparable to our best ML estimates. By contrast, our new fasttree approach with MP starting trees using the full dataset provided a strong alternative to RAxML-NG, delivering similar topological accuracy and branch length estimates with a substantially reduced computational burden. Using this approach, replicate analyses to test different MP starting trees and models is also computationally efficient, and simple criteria, such as likelihood values, can be used to

assess the resulting trees for those taxonomic groups that lack sufficient study to define expected clades. Thus, the new fasttree approach we used can be broadly applicable to any taxonomic group. By demonstrating the feasibility of computationally efficient methods, this study offers a roadmap for constructing large-scale phylogenies across the Tree of Life.

### Data Availability

All the original data (accessions, alignments, summary statistics, taxon subsets, summary of all fasttree runs, clade ages and tree files) and scripts necessary to reproduce the analyses reported in this study can be accessed through the Dryad link:

https://doi.org/10.5061/dryad.5dv41nsgw.

### **Acknowledgements**

We thank Bui Quang Minh for insights on the fasttree approach using IQ-TREE and Siavash Mirarab and Chao Zhang for advice on running large ASTRAL trees. We thank Jeremy Kirchman, Zongji Wang, and Qi Zhou for sharing tree files. We also thank J. Klicka, M. Ahmad, W. Tsai Nakashima, and E.M. Smith for support. Portions of this research were conducted with high-performance computing resources provided by Louisiana State University (http://www.hpc.lsu.edu). This work was supported by National Science Foundation grant DEB-1655624 (BCF and RTB), DEB-2217442 (BCF and RTB - supplement), DEB-1655736 (BTS), DEB-1655683 (ELB and RTK), DEB-2203216 (MGH, EPD, and RTB), and Villum Fonden 25925 (PAH). Part of this work was funded by UKRI grant MR/X015130/1. For the purpose of open access, the authors have applied a Creative Commons Attribution (CC BY) license to any Author Accepted Manuscript version arising. We thank Bob Thomson, Marek Borowiec, and an anonymous reviewer for their valuable comments that improved this manuscript. We also thank Bob Thomson for relaying details of a discussion regarding the possible effects of differences in the resolution of taxonomic backbones on supertree methods that we incorporated to the text.

806	Disclaimer
807	Any use of trade, firm, or product names is for descriptive purposes only and does not imply
808	endorsement by the U.S. Government.
809	
810	Reference
811	Andermann T, Fernandes AM, Olsson U, Töpel M, Pfeil B, Oxelman B, Aleixo A, Faircloth BC,
812	Antonelli A. 2019. Allele phasing greatly improves the phylogenetic utility of ultraconserved
813	elements. Syst. Biol. 68:32–46. DOI: 10.1093/sysbio/syy039
814	Andersen MJ, McCullough JM, Friedman NR, Peterson AT, Moyle RG, Joseph L, Nyári ÁS. 2019.
815	Ultraconserved elements resolve genus-level relationships in a major Australasian bird
816	radiation (Aves: Meliphagidae). Emu - Austral Ornithology 119:218–232. DOI:
817	10.1080/01584197.2019.1595662
818	Andersen MJ, McCullough JM, Mauck WM, Smith BT, Moyle RG. 2018. A phylogeny of
819	kingfishers reveals an Indomalayan origin and elevated rates of diversification on oceanic
820	islands. J. Biogeogr. 45:269–281. DOI: 10.1111/jbi.13139
821	Bader DA, Roshan U, Stamatakis A. 2006. Computational grand challenges in assembling the
822	tree of life: problems and solutions. In: Computational biology and bioinformatics. Vol. 68.
823	Advances in Computers. Elsevier. p. 127–176. DOI: 10.1016/S0065-2458(06)68004-2
824	Baker WJ, Savolainen V, Asmussen-Lange CB, Chase MW, Dransfield J, Forest F, Harley MM, Uhl
825	NW, Wilkinson M. 2009. Complete generic-level phylogenetic analyses of palms
826	(Arecaceae) with comparisons of supertree and supermatrix approaches. Syst. Biol.
827	58:240–256. DOI: 10.1093/sysbio/syp021
828	Baum BR. 1992. Combining trees as a way of combining data sets for phylogenetic inference,
829	and the desirability of combining gene trees. Taxon 41:3–10. DOI: 10.2307/1222480
830	Bininda-Emonds OR, Gittleman JL, Purvis A. 1999. Building large trees by combining
831	phylogenetic information: a complete phylogeny of the extant Carnivora (Mammalia). Biol.
832	Rev. Camb. Philos. Soc. 74:143–175. DOI: 10.1017/s0006323199005307
833	Bininda-Emonds OR, Sanderson MJ. 2001. Assessment of the accuracy of matrix representation

834	with parsimony analysis supertree construction. Syst. Biol. 50:565–579. DOI:
835	10.1080/10635150120358
836	Bininda-Emonds ORP, Gittleman JL, Steel MA. 2002. The (Super)Tree of Life: Procedures,
837	Problems, and Prospects. Annu. Rev. Ecol. Syst. 33:265–289. DOI:
838	10.1146/annurev.ecolsys.33.010802.150511
839	Bininda-Emonds ORP. 2004. The evolution of supertrees. Trends Ecol. Evol. 19:315–322. DOI:
840	10.1016/j.tree.2004.03.015
841	Bolton, B. 2025. AntCat – An online catalog of the ants of the world. Available from
842	https://antcat.org. (accessed Sept 3, 2025)
843	Borowiec ML. 2016. AMAS: a fast tool for alignment manipulation and computing of summary
844	statistics. PeerJ 4:e1660. DOI: 10.7717/peerj.1660
845	Borowiec ML, Zhang YM, Neves K, Ramalho MO, Fisher BL, Lucky A, Moreau CS. 2025.
846	Evaluating UCE Data Adequacy and Integrating Uncertainty in a Comprehensive Phylogeny
847	of Ants. Syst. Biol. syaf001. DOI: 10.1093/sysbio/syaf001
848	Braun EL, Cracraft J, Houde P. 2019. Resolving the Avian Tree of Life from Top to Bottom: The
849	Promise and Potential Boundaries of the Phylogenomic Era. In: Kraus RHS, editor. Avian
850	Genomics in Ecology and Evolution: From the Lab into the Wild. Cham: Springer
851	International Publishing. p. 151–210. DOI: 10.1007/978-3-030-16477-5_6
852	Braun EL, Oliveros CH, White Carreiro ND, Zhao M, Glenn TC, Brumfield RT, Braun MJ, Kimball
853	RT, Faircloth BC. 2024. Testing the mettle of METAL: A comparison of phylogenomic
854	methods using a challenging but well-resolved phylogeny. BioRxiv. DOI:
855	10.1101/2024.02.28.582627
856	Brocklehurst N, Field DJ. 2024. Tip dating and Bayes factors provide insight into the divergences
857	of crown bird clades across the end-Cretaceous mass extinction. Proc. Biol. Sci.
858	291:20232618. DOI: 10.1098/rspb.2023.2618
859	Bruxaux J, Gabrielli M, Ashari H, Prŷs-Jones R, Joseph L, Milá B, Besnard G, Thébaud C. 2018.
860	Recovering the evolutionary history of crowned pigeons (Columbidae: Goura): Implications
861	for the biogeography and conservation of New Guinean lowland birds. Mol. Phylogenet.
862	Evol. 120:248–258. DOI: 10.1016/j.ympev.2017.11.022

863	Bryson RW, Faircloth BC, Tsai WLE, McCormack JE, Klicka J. 2016. Target enrichment of
864	thousands of ultraconserved elements sheds new light on early relationships within New
865	World sparrows (Aves: Passerellidae). Auk 133:451–458. DOI: 10.1642/AUK-16-26.1
866	Burga A, Wang W, Ben-David E, Wolf PC, Ramey AM, Verdugo C, Lyons K, Parker PG, Kruglyak L
867	2017. A genetic signature of the evolution of loss of flight in the Galapagos cormorant.
868	Science 356. DOI: 10.1126/science.aal3345
869	Burleigh JG, Kimball RT, Braun EL. 2015. Building the avian tree of life using a large-scale, sparse
870	supermatrix. Mol. Phylogenet. Evol. 84:53–63. DOI: 10.1016/j.ympev.2014.12.003
871	Campillo LC, Oliveros CH, Sheldon FH, Moyle RG. 2018. Genomic data resolve gene tree
872	discordance in spiderhunters (Nectariniidae, Arachnothera). Mol. Phylogenet. Evol.
873	120:151–157. DOI: 10.1016/j.ympev.2017.12.011
874	Capella-Gutiérrez S, Silla-Martínez JM, Gabaldón T. 2009. trimAl: A tool for automated
875	alignment trimming in large-scale phylogenetic analyses. Bioinformatics 25:1972–1973.
876	DOI: 10.1093/bioinformatics/btp348
877	Catanach TA, Halley MR, Allen JM, Johnson JA, Thorstrom R, Palhano S, Poor Thunder C,
878	Gallardo JC, Weckstein JD. 2021. Systematics and conservation of an endemic radiation of
879	Accipiter hawks in the Caribbean islands. Ornithology 138. DOI:
880	10.1093/ornithology/ukab041
881	Chen A, Field DJ. 2020. Phylogenetic definitions for Caprimulgimorphae (Aves) and major
882	constituent clades under the International Code of Phylogenetic Nomenclature. Vertebr.
883	Zool. 70:571–585. DOI: 10.26049/VZ70-4-2020-03
884	Chen D, Braun EL, Forthman M, Kimball RT, Zhang Z. 2018. A simple strategy for recovering
885	ultraconserved elements, exons, and introns from low coverage shotgun sequencing of
886	museum specimens: Placement of the partridge genus Tropicoperdix within the
887	Galliformes. Mol. Phylogenet. Evol. 129:304–314. DOI: 10.1016/j.ympev.2018.09.005
888	Claramunt S, Braun EL, Cracraft J, Fjeldså J, Ho SYW, Houde P, Nguyen JMT, Stiller J. 2024.
889	Calibrating the genomic clock of modern birds using fossils. Proc Natl Acad Sci USA
890	121:e2405887121. DOI: 10.1073/pnas.2405887121
891	Claramunt S, Cracraft J. 2015. A new time tree reveals Earth history's imprint on the evolution

892	of modern birds. Sci. Adv. 1:e1501005. DOI: 10.1126/sciadv.1501005
893	Clements JF, Rasmussen PC, Schulenberg TS, Iliff MJ, Fredericks TA, Gerbracht JA, Lepage D,
894	Spencer A, Billerman SM, Sullivan BL, Wood CL. 2023. The eBird/Clements checklist of Birds
895	of the World: v2023. Available from:
896	https://www.birds.cornell.edu/clementschecklist/download/
897	Cotton JA, Wilkinson M. 2009. Supertrees join the mainstream of phylogenetics. Trends Ecol.
898	Evol. 24:1–3. DOI: 10.1016/j.tree.2008.08.006
899	Cracraft J, Donoghue MJ. 2004. Assembling the tree of life. Oxford University Press
900	Creevey CJ, McInerney JO. 2005. Clann: investigating phylogenetic information through
901	supertree analyses. Bioinformatics 21:390–392. DOI: 10.1093/bioinformatics/bti020
902	Delsuc F, Brinkmann H, Philippe H. 2005. Phylogenomics and the reconstruction of the tree of
903	life. Nat. Rev. Genet. 6:361–375. DOI: 10.1038/nrg1603
904	Dickinson EC, Christidis L eds. 2014. The Howard and Moore Complete Checklist of the Birds of
905	the World Fourth Edition. Eastbourne: Aves Press
906	Driskell AC, Ané C, Burleigh JG, McMahon MM, O'meara BC, Sanderson MJ. 2004. Prospects for
907	building the tree of life from large sequence databases. Science 306:1172–1174. DOI:
908	10.1126/science.1102036
909	Dwivedi B, Gadagkar SR. 2009. Phylogenetic inference under varying proportions of indel-
910	induced alignment gaps. BMC Evol. Biol. 9:211. DOI: 10.1186/1471-2148-9-211
911	Everson KM, McLaughlin JF, Cato IA, Evans MM, Gastaldi AR, Mills KK, Shink KG, Wilbur SM,
912	Winker K. 2019. Speciation, gene flow, and seasonal migration in Catharus thrushes
913	(Aves:Turdidae). Mol. Phylogenet. Evol. 139:106564. DOI: 10.1016/j.ympev.2019.106564
914	Faircloth BC, McCormack JE, Crawford NG, Harvey MG, Brumfield RT, Glenn TC. 2012.
915	Ultraconserved elements anchor thousands of genetic markers spanning multiple
916	evolutionary timescales. Syst. Biol. 61:717–726. DOI: 10.1093/sysbio/sys004
917	Faircloth BC. 2016. PHYLUCE is a software package for the analysis of conserved genomic loci.
918	Bioinformatics 32:786–788. DOI: 10.1093/bioinformatics/btv646
919	Felsenstein J. 1985. Confidence limits on phylogenies: an approach using the bootstrap.
920	Evolution 39:783–791, DOI: 10.2307/2408678

921	Ferreira M, Fernandes AM, Aleixo A, Antonelli A, Olsson U, Bates JM, Cracraft J, Ribas CC. 2018.
922	Evidence for mtDNA capture in the jacamar Galbula leucogastra/chalcothorax species-
923	complex and insights on the evolution of white-sand ecosystems in the Amazon basin. Mol.
924	Phylogenet. Evol. 129:149–157. DOI: 10.1016/j.ympev.2018.07.007
925	Field DJ, Benito J, Chen A, Jagt JWM, Ksepka DT. 2020. Late Cretaceous neornithine from
926	Europe illuminates the origins of crown birds. Nature 579:397–401. DOI: 10.1038/s41586-
927	020-2096-0
928	Gascuel O. 1997. BIONJ: an improved version of the NJ algorithm based on a simple model of
929	sequence data. Mol. Biol. Evol. 14:685–695. DOI: 10.1093/oxfordjournals.molbev.a025808
930	Gatesy J, Baker RH, Hayashi C. 2004. Inconsistencies in arguments for the supertree approach:
931	supermatrices versus supertrees of Crocodylia. Syst. Biol. 53:342–355. DOI:
932	10.1080/10635150490423971
933	Gill F, Donsker D, Rasmussen P. 2023. IOC World Bird List (v 13.1). Available from:
934	http://dx.doi.org/10.14344/IOC.ML.13.1
935	Goloboff PA, Catalano SA, Marcos Mirande J, Szumik CA, Salvador Arias J, Källersjö M, Farris JS.
936	2009. Phylogenetic analysis of 73 060 taxa corroborates major eukaryotic groups. Cladistics
937	25:211–230. DOI: 10.1111/j.1096-0031.2009.00255.x
938	Gu Z. 2022. Complex heatmap visualization. iMeta 1:e43. DOI: 10.1002/imt2.43
939	Hackett SJ, Kimball RT, Reddy S, Bowie RCK, Braun EL, Braun MJ, Chojnowski JL, Cox WA, Han
940	KL, Harshman J, Huddleston CJ. 2008. A phylogenomic study of birds reveals their
941	evolutionary history. Science 320:1763–1768. DOI: 10.1126/science.1157704
942	Harvey MG, Bravo GA, Claramunt S, Cuervo AM, Derryberry GE, Battilana J, Seeholzer GF,
943	McKay JS, O'Meara BC, Faircloth BC, Edwards SV. 2020. The evolution of a tropical
944	biodiversity hotspot. Science 370:1343–1348. DOI: 10.1126/science.aaz6970
945	Hinchliff CE, Smith SA, Allman JF, Burleigh JG, Chaudhary R, Coghill LM, Crandall KA, Deng J,
946	Drew BT, Gazis R, Gude K, Hibbett DS, Katz LA, Laughinghouse HD, McTavish EJ, Midford PE,
947	Owen CL, Ree RH, Rees JA, Soltis DE, Williams T, Cranston KA. 2015. Synthesis of phylogeny
948	and taxonomy into a comprehensive tree of life. Proc Natl Acad Sci USA 112:12764–12769.
0/0	DOI: 10.1073/ppas 1423041112

950	Hosner PA, Faircloth BC, Glenn TC, Braun EL, Kimball RT. 2016. Avoiding missing data biases in
951	phylogenomic inference: an empirical study in the landfowl (Aves: Galliformes). Mol. Biol.
952	Evol. 33:1110–1125. DOI: 10.1093/molbev/msv347
953	Huerta-Cepas J, Serra F, Bork P. 2016. ETE 3: reconstruction, analysis, and visualization of
954	phylogenomic data. Mol. Biol. Evol. 33:1635–1638. DOI: 10.1093/molbev/msw046
955	Imfeld TS, Barker FK, Brumfield RT. 2020. Mitochondrial genomes and thousands of
956	ultraconserved elements resolve the taxonomy and historical biogeography of the
957	Euphonia and Chlorophonia finches (Passeriformes: Fringillidae). Auk 137. DOI:
958	10.1093/auk/ukaa016
959	Jarvis ED, Mirarab S, Aberer AJ, Li B, Houde P, Li C, Ho SYW, Faircloth BC, Nabholz B, Howard JT,
960	Suh A, Weber CC, da Fonseca RR, Li J, Zhang F, Li H, Zhou L, Narula N, Liu L, Ganapathy G,
961	Boussau B, Bayzid MS, Zavidovych V, Subramanian S, Gabaldón T, Capella-Gutiérrez S,
962	Huerta-Cepas J, Rekepalli B, Munch K, Schierup M, Lindow B, Warren WC, Ray D, Green RE,
963	Bruford MW, Zhan X, Dixon A, Li S, Li N, Huang Y, Derryberry EP, Bertelsen MF, Sheldon FH,
964	Brumfield RT, Mello CV, Lovell PV, Wirthlin M, Cruz Schneider MP, Prosdocimi F, Samaniego
965	JA, Vargas Velazquez AM, Alfaro-Núñez A, Campos PF, Petersen B, Sicheritz-Ponten T, Pas
966	A, Bailey T, Scofield P, Bunce M, Lambert DM, Zhou Q, Perelman P, Driskell AC, Shapiro B,
967	Xiong Z, Zeng Y, Liu S, Li Z, Liu B, Wu K, Xiao J, Yinqi X, Zheng Q, Zhang Y, Yang H, Wang J,
968	Smeds L, Rheindt FE, Braun M, Fjeldsa J, Orlando L, Barker FK, Jønsson KA, Johnson W,
969	Koepfli K-P, O'Brien S, Haussler D, Ryder OA, Rahbek C, Willerslev E, Graves GR, Glenn TC,
970	McCormack J, Burt D, Ellegren H, Alström P, Edwards SV, Stamatakis A, Mindell DP, Cracraft
971	J, Braun EL, Warnow T, Jun W, Gilbert MTP, Zhang G. 2014. Whole-genome analyses
972	resolve early branches in the tree of life of modern birds. Science 346:1320–1331. DOI:
973	10.1126/science.1253451
974	Jetz W, Thomas GH, Joy JB, Hartmann K, Mooers AO. 2012. The global diversity of birds in space
975	and time. Nature 491:444–448. DOI: 10.1038/nature11631
976	Kapli P, Yang Z, Telford MJ. 2020. Phylogenetic tree building in the genomic age. Nat. Rev.
977	Genet. 21:428–444. DOI: 10.1038/s41576-020-0233-0
978	Katoh K, Standley DM. 2013. MAFFT multiple sequence alignment software version 7:

979	improvements in performance and usability. Mol. Biol. Evol. 30:772–780. DOI:
980	10.1093/molbev/mst010
981	Kimball RT, Braun EL, Barker FK, Bowie RCK, Braun MJ, Chojnowski JL, Hackett SJ, Han K-L,
982	Harshman J, Heimer-Torres V, Holznagel W, Huddleston CJ, Marks BD, Miglia KJ, Moore
983	WS, Reddy S, Sheldon FH, Smith JV, Witt CC, Yuri T. 2009. A well-tested set of primers to
984	amplify regions spread across the avian genome. Mol. Phylogenet. Evol. 50:654–660. DOI:
985	10.1016/j.ympev.2008.11.018
986	Kimball RT, Oliveros CH, Wang N, White ND, Barker FK, Field DJ, Ksepka DT, Chesser RT, Moyle
987	RG, Braun MJ, Brumfield RT, Faircloth BC, Smith BT, Braun EL. 2019. A phylogenomic
988	supertree of birds. Diversity 11:109. DOI: 10.3390/d11070109
989	Kirchman JJ, Rotzel McInerney N, Giarla TC, Olson SL, Slikas E, Fleischer RC. 2021. Phylogeny
990	based on ultra-conserved elements clarifies the evolution of rails and allies (Ralloidea) and
991	is the basis for a revised classification. Ornithology 138. DOI: 10.1093/ornithology/ukab042
992	Koonin EV. 2005. Orthologs, paralogs, and evolutionary genomics. Annu. Rev. Genet. 39:309–
993	338. DOI: 10.1146/annurev.genet.39.073003.114725
994	Kozlov AM, Darriba D, Flouri T, Morel B, Stamatakis A. 2019. RAxML-NG: a fast, scalable and
995	user-friendly tool for maximum likelihood phylogenetic inference. Bioinformatics 35:4453–
996	4455. DOI: 10.1093/bioinformatics/btz305
997	Kuhl H, Frankl-Vilches C, Bakker A, Mayr G, Nikolaus G, Boerno ST, Klages S, Timmermann B,
998	Gahr M. 2021. An Unbiased Molecular Approach Using 3'-UTRs Resolves the Avian Family-
999	Level Tree of Life. Mol. Biol. Evol. 38:108–127. DOI: 10.1093/molbev/msaa191
1000	Lamichhaney S, Berglund J, Almén MS, Maqbool K, Grabherr M, Martinez-Barrio A, Promerová
1001	M, Rubin C-J, Wang C, Zamani N, Grant BR, Grant PR, Webster MT, Andersson L. 2015.
1002	Evolution of Darwin's finches and their beaks revealed by genome sequencing. Nature
1003	518:371–375. DOI: 10.1038/nature14181
1004	Lê S, Josse J, Husson F. 2008. FactoMineR: An R package for multivariate analysis. J. Stat. Softw.
1005	25. DOI: 10.18637/jss.v025.i01
1006	Leite RN, Kimball RT, Braun EL, Derryberry EP, Hosner PA, Derryberry GE, Anciães M, McKay JS,
1007	Aleivo A Rihas CC Brumfield RT Cracraft I 2021 Phylogenomics of manakins (Aves:

1008	Pipridae) using alternative locus filtering strategies based on informativeness. Mol.
1009	Phylogenet. Evol. 155:107013. DOI: 10.1016/j.ympev.2020.107013
1010	Liu FG, Miyamoto MM, Freire NP, Ong PQ, Tennant MR, Young TS, Gugel KF. 2001. Molecular
1011	and morphological supertrees for eutherian (placental) mammals. Science 291:1786–1789.
1012	DOI: 10.1126/science.1056346
1013	Liu L, Yu L, Edwards SV. 2010. A maximum pseudo-likelihood approach for estimating species
1014	trees under the coalescent model. BMC Evol. Biol. 10:302. DOI: 10.1186/1471-2148-10-302
1015	Manthey JD, Campillo LC, Burns KJ, Moyle RG. 2016. Comparison of Target-Capture and
1016	Restriction-Site Associated DNA Sequencing for Phylogenomics: A Test in Cardinalid
1017	Tanagers (Aves, Genus: Piranga). Syst. Biol. 65:640–650. DOI: 10.1093/sysbio/syw005
1018	McCormack JE, Harvey MG, Faircloth BC, Crawford NG, Glenn TC, Brumfield RT. 2013. A
1019	phylogeny of birds based on over 1,500 loci collected by target enrichment and high-
1020	throughput sequencing. PLoS ONE 8:e54848. DOI: 10.1371/journal.pone.0054848
1021	McCormack JE, Hird SM, Zellmer AJ, Carstens BC, Brumfield RT. 2013. Applications of next-
1022	generation sequencing to phylogeography and phylogenetics. Mol. Phylogenet. Evol.
1023	66:526–538. DOI: 10.1016/j.ympev.2011.12.007
1024	McCormack JE, Tsai WLE, Faircloth BC. 2016. Sequence capture of ultraconserved elements
1025	from bird museum specimens. Mol. Ecol. Resour 16:1189–1203. DOI: 10.1111/1755-
1026	0998.12466
1027	McCullough JM., Joseph L, Moyle RG, Andersen MJ. 2019a. Ultraconserved elements put the
1028	final nail in the coffin of traditional use of the genus Meliphaga (Aves: Meliphagidae). Zool.
1029	Scr. 48:411–418. DOI: 10.1111/zsc.12350
1030	McCullough JM, Moyle RG, Smith BT, Andersen MJ. 2019b. A Laurasian origin for a pantropical
1031	bird radiation is supported by genomic and fossil data (Aves: Coraciiformes). Proc. Biol. Sci.
1032	286:20190122. DOJ: 10.1098/rspb.2019.0122
1033	McCullough JM, Oliveros CH, Benz BW, Zenil-Ferguson R, Cracraft J, Moyle RG, Andersen MJ.
1034	2022. Wallacean and Melanesian Islands Promote Higher Rates of Diversification within the
1035	Global Passerine Radiation Corvides. Syst. Biol. 71:1423–1439. DOI:
1036	10.1093/sysbio/syac044

1037	McTavish EJ, Gerbracht JA, Holder MT, IIIff MJ, Lepage D, Rasmussen P, Redelings B, Sanchez
1038	Reyes LL, Miller ET. 2024. A complete and dynamic tree of birds. Proc Natl Acad Sci USA
1039	122: e2409658122. DOI: 10.1073/pnas.2409658122
1040	Minh BQ, Schmidt HA, Chernomor O, Schrempf D, Woodhams MD, von Haeseler A, Lanfear R.
1041	2020. IQ-TREE 2: New models and efficient methods for phylogenetic inference in the
1042	genomic era. Mol. Biol. Evol. 37:1530–1534. DOI: 10.1093/molbev/msaa015
1043	Mitchell KJ, Cooper A, Phillips MJ. 2015. Comment on "Whole-genome analyses resolve early
1044	branches in the tree of life of modern birds". Science 349:1460. DOI:
1045	10.1126/science.aab1062
1046	Moore B, Smith S, Donoghue M. 2006. Increasing Data Transparency and Estimating
1047	Phylogenetic Uncertainty in Supertrees: Approaches Using Nonparametric Bootstrapping.
1048	Syst. Biol. 55:662–676. DOI: 10.1080/10635150600920693
1049	Moyle RG, Oliveros CH, Andersen MJ, Hosner PA, Benz BW, Manthey JD, Travers SL, Brown RM,
1050	Faircloth BC. 2016. Tectonic collision and uplift of Wallacea triggered the global songbird
1051	radiation. Nat. Commun. 7:12709. DOI: 10.1038/ncomms12709
1052	Musher LJ, Cracraft J. 2018. Phylogenomics and species delimitation of a complex radiation of
1053	Neotropical suboscine birds ( <i>Pachyramphus</i> ). Mol. Phylogenet. Evol. 118:204–221. DOI:
1054	10.1016/j.ympev.2017.09.013
1055	Nater A, Burri R, Kawakami T, Smeds L, Ellegren H. 2015. Resolving Evolutionary Relationships in
1056	Closely Related Species with Whole-Genome Sequencing Data. Syst. Biol. 64:1000–1017.
1057	DOI: 10.1093/sysbio/syv045
1058	Nguyen L-T, Schmidt HA, von Haeseler A, Minh BQ. 2015. IQ-TREE: a fast and effective
1059	stochastic algorithm for estimating maximum-likelihood phylogenies. Mol. Biol. Evol.
1060	32:268–274. DOI: 10.1093/molbev/msu300
1061	Nixon K. 1999. The parsimony ratchet, a new method for rapid parsimony analysis. Cladistics
1062	15:407-414. DOI: 10.1111/j.1096-0031.1999.tb00277.x
1063	Nyakatura K, Bininda-Emonds ORP. 2012. Updating the evolutionary history of Carnivora
1064	(Mammalia): a new species-level supertree complete with divergence time estimates. BMC
1065	Biol. 10:12. DOI: 10.1186/1741-7007-10-12

1066	Ogden TH, Rosenberg MS. 2006. Multiple sequence alignment accuracy and phylogenetic
1067	inference. Syst. Biol. 55:314–328. DOI: 10.1080/10635150500541730
1068	Oliveros CH, Andersen MJ, Hosner PA, Mauck WM, Sheldon FH, Cracraft J, Moyle RG. 2020.
1069	Rapid Laurasian diversification of a pantropical bird family during the Oligocene–Miocene
1070	transition. Ibis 162:137–152. DOI: 10.1111/ibi.12707
1071	Oliveros CH, Andersen MJ, Moyle RG. 2021. A phylogeny of white-eyes based on ultraconserved
1072	elements. Mol. Phylogenet. Evol. 164:107273. DOI: 10.1016/j.ympev.2021.107273
1073	Oliveros CH, Field DJ, Ksepka DT, Barker FK, Aleixo A, Andersen MJ, Alström P, Benz BW, Braun
1074	EL, Braun MJ, Bravo GA, Brumfield RT, Chesser RT, Claramunt S, Cracraft J, Cuervo AM,
1075	Derryberry EP, Glenn TC, Harvey MG, Hosner PA, Joseph L, Kimball RT, Mack AL, Miskelly
1076	CM, Peterson AT, Robbins MB, Sheldon FH, Silveira LF, Smith BT, White ND, Moyle RG,
1077	Faircloth BC. 2019. Earth history and the passerine superradiation. Proc Natl Acad Sci USA
1078	116:7916–7925. DOI: 10.1073/pnas.1813206116
1079	Ottenburghs J, Megens H-J, Kraus RHS, Madsen O, van Hooft P, van Wieren SE, Crooijmans
1080	RPMA, Ydenberg RC, Groenen MAM, Prins HHT. 2016. A tree of geese: A phylogenomic
1081	perspective on the evolutionary history of True Geese. Mol. Phylogenet. Evol. 101:303–
1082	313. DOI: 10.1016/j.ympev.2016.05.021
1083	Pacheco MA, Battistuzzi FU, Lentino M, Aguilar RF, Kumar S, Escalante AA. 2011. Evolution of
1084	modern birds revealed by mitogenomics: timing the radiation and origin of major orders.
1085	Mol. Biol. Evol. 28:1927–1942. DOI: 10.1093/molbev/msr014
1086	Paradis E, Schliep K. 2019. ape 5.0: an environment for modern phylogenetics and evolutionary
1087	analyses in R. Bioinformatics 35:526–528. DOI: 10.1093/bioinformatics/bty633
1088	Parham JF, Donoghue PCJ, Bell CJ, Calway TD, Head JJ, Holroyd PA, Inoue JG, Irmis RB, Joyce
1089	WG, Ksepka DT, Patané JSL, Smith ND, Tarver JE, van Tuinen M, Yang Z, Angielczyk KD,
1090	Greenwood JM, Hipsley CA, Jacobs L, Makovicky PJ, Müller J, Smith KT, Theodor JM,
1091	Warnock RCM, Benton MJ. 2012. Best practices for justifying fossil calibrations. Syst. Biol.
1092	61:346–359. DOI: 10.1093/sysbio/syr107
1093	Philippe H, Brinkmann H, Lavrov DV, Littlewood DTJ, Manuel M, Wörheide G, Baurain D. 2011.
1094	Resolving difficult phylogenetic questions; why more sequences are not enough. PLoS Biol.

1095	9:e1000602. DOI: 10.1371/Journal.pbi0.1000602
1096	Philippe H, Snell EA, Bapteste E, Lopez P, Holland PWH, Casane D. 2004. Phylogenomics of
1097	eukaryotes: impact of missing data on large alignments. Mol. Biol. Evol. 21:1740–1752.
1098	DOI: 10.1093/molbev/msh182
1099	Portik DM, Wiens JJ. 2021. Do Alignment and Trimming Methods Matter for Phylogenomic
1100	(UCE) Analyses? Syst. Biol. 70: 440–462. DOI: 10.1093/sysbio/syaa064
1101	Price MN, Dehal PS, Arkin AP. 2010. FastTree 2 — approximately maximum-likelihood trees for
1102	large alignments. PLoS ONE 5:e9490. DOI: 10.1371/journal.pone.0009490
1103	Prum RO, Berv JS, Dornburg A, Field DJ, Townsend JP, Lemmon EM, Lemmon AR. 2015. A
1104	comprehensive phylogeny of birds (Aves) using targeted next-generation DNA sequencing.
1105	Nature 526:569–573. DOI: 10.1038/nature15697
1106	Purvis A. 1995. A composite estimate of primate phylogeny. Philos. Trans. R. Soc. Lond. B Biol.
1107	Sci. 348:405–421. DOI: 10.1098/rstb.1995.0078
1108	Queiroz K de, Cantino PD, Gauthier JA. 2020. Phylonyms: A companion to the phylocode. (de
1109	Queiroz K, Cantino P, Gauthier J, editors.). Boca Raton: CRC Press
1110	Ragan MA. 1992. Phylogenetic inference based on matrix representation of trees. Mol.
1111	Phylogenet. Evol. 1:53–58. DOI: 10.1016/1055-7903(92)90035-F
1112	Reddy S, Kimball RT, Pandey A, Hosner PA, Braun MJ, Hackett SJ, Han K-L, Harshman J,
1113	Huddleston CJ, Kingston S, Marks BD, Miglia KJ, Moore WS, Sheldon FH, Witt CC, Yuri T,
1114	Braun EL. 2017. Why Do Phylogenomic Data Sets Yield Conflicting Trees? Data Type
1115	Influences the Avian Tree of Life more than Taxon Sampling. Syst. Biol. 66:857–879. DOI:
1116	10.1093/sysbio/syx041
1117	Redelings BD, Holder MT. 2017. A supertree pipeline for summarizing phylogenetic and
1118	taxonomic information for millions of species. PeerJ 5:e3058. DOI: 10.7717/peerj.3058
1119	Robinson DF, Foulds LR. 1981. Comparison of phylogenetic trees. Math. Biosci. 53:131–147.
1120	DOI: 10.1016/0025-5564(81)90043-2
1121	R Core Team. 2023. R: A language and environment for statistical computing. Vienna, Austria: R
1122	Foundation for Statistical Computing
1123	Sackton TB, Grayson P, Cloutier A, Hu Z, Liu JS, Wheeler NE, Gardner PP, Clarke JA, Baker AJ,

1124	Clamp M, Edwards SV. 2019. Convergent regulatory evolution and loss of flight in
1125	paleognathous birds. Science 364:74–78. DOI: 10.1126/science.aat7244
1126	Salter JF, Oliveros CH, Hosner PA, Manthey JD, Robbins MB, Moyle RG, Brumfield RT, Faircloth
1127	BC. 2020. Extensive paraphyly in the typical owl family (Strigidae). Auk 137. DOI:
1128	10.1093/auk/ukz070
1129	Sanderson MJ, McMahon MM, Steel M. 2010. Phylogenomics with incomplete taxon coverage:
1130	the limits to inference. BMC Evol. Biol. 10:155. DOI: 10.1186/1471-2148-10-155
1131	Sanderson MJ, Purvis A, Henze C. 1998. Phylogenetic supertrees: Assembling the trees of life.
1132	Trends Ecol. Evol. 13:105–109. DOI: 10.1016/S0169-5347(97)01242-1
1133	Sangster G, Braun EL, Johansson US, Kimball RT, Mayr G, Suh A. 2022. Phylogenetic definitions
1134	for 25 higher-level clade names of birds. Avian Res.:100027. DOI:
1135	10.1016/j.avrs.2022.100027
1136	Sangster G, Mayr G. 2021. Feraequornithes: a name for the clade formed by Procellariiformes,
1137	Sphenisciformes, Ciconiiformes, Suliformes and Pelecaniformes (Aves). Vertebr. Zool.
1138	71:49–53. DOI: 10.3897/vz.71.e61728
1139	Schliep KP. 2011. phangorn: phylogenetic analysis in R. Bioinformatics 27:592–593. DOI:
1140	10.1093/bioinformatics/btq706
1141	Schwery O, O'Meara BC. 2016. MonoPhy: a simple R package to find and visualize monophyly
1142	issues. PeerJ Computer Science 2:e56. DOI: 10.7717/peerj-cs.56
1143	Smith BT, Harvey MG, Faircloth BC, Glenn TC, Brumfield RT. 2014. Target capture and massively
1144	parallel sequencing of ultraconserved elements for comparative studies at shallow
1145	evolutionary time scales. Syst. Biol. 63:83–95. DOI: 10.1093/sysbio/syt061
1146	Smith BT, Mauck WM, Benz BW, Andersen MJ. 2020. Uneven Missing Data Skew Phylogenomic
1147	Relationships within the Lories and Lorikeets. Genome Biol. Evol. 12:1131–1147. DOI:
1148	10.1093/gbe/evaa113
1149	Smith BT, Merwin J, Provost KL, Thom G, Brumfield RT, Ferreira M, Mauck WM, Moyle RG,
1150	Wright TF, Joseph L. 2023. Phylogenomic Analysis of the Parrots of the World Distinguishes
1151	Artifactual from Biological Sources of Gene Tree Discordance. Syst. Biol. 72:228–241. DOI:
1152	10.1093/cychio/cyac055

1153	Smith SA, O'Meara BC. 2012. treePL: Divergence time estimation using penalized likelihood for
1154	large phylogenies. Bioinformatics 28:2689–2690. DOI: 10.1093/bioinformatics/bts492
1155	Springer MS, Gatesy J. 2014. Land plant origins and coalescence confusion. Trends Plant Sci.
1156	19:267–269. DOI: 10.1016/j.tplants.2014.02.012
1157	Stiller J, Feng S, Chowdhury AA, Rivas-González I, Duchêne DA, Fang Q, Deng Y, Kozlov A,
1158	Stamatakis A, Claramunt S, Nguyen JMT, Ho SYW, Faircloth BC, Haag J, Houde P, Cracraft J,
1159	Balaban M, Mai U, Chen G, Gao R, Zhou C, Xie Y, Huang Z, Cao Z, Yan Z, Ogilvie HA, Nakhleh
1160	L, Lindow B, Morel B, Fjeldså J, Hosner PA, da Fonseca RR, Petersen B, Tobias JA, Székely T,
1161	Kennedy JD, Reeve AH, Liker A, Stervander M, Antunes A, Tietze DT, Bertelsen MF, Lei F,
1162	Rahbek C, Graves GR, Schierup MH, Warnow T, Braun EL, Gilbert MTP, Jarvis ED, Mirarab S
1163	Zhang G. 2024. Complexity of avian evolution revealed by family-level genomes. Nature
1164	629:851–860. DOI: 10.1038/s41586-024-07323-1
1165	Sukumaran J, Holder MT. 2010. DendroPy: a Python library for phylogenetic computing.
1166	Bioinformatics 26:1569–1571.
1167	Sun K, Meiklejohn KA, Faircloth BC, Glenn TC, Braun EL, Kimball RT. 2014. The evolution of
1168	peafowl and other taxa with ocelli (eyespots): a phylogenomic approach. Proc. Biol. Sci.
1169	281. DOI: 10.1098/rspb.2014.0823
1170	Swofford DL. 2003. PAUP* Phylogenetic Analysis Using Parsimony (*and Other Methods).
1171	Version 4. http://paup.csit.fsu.edu/.
1172	Tan G, Muffato M, Ledergerber C, Herrero J, Goldman N, Gil M, Dessimoz C. 2015. Current
1173	Methods for Automated Filtering of Multiple Sequence Alignments Frequently Worsen
1174	Single-Gene Phylogenetic Inference. Syst. Biol. 64:778–791. DOI: 10.1093/sysbio/syv033
1175	Title PO, Rabosky DL. 2017. Do Macrophylogenies Yield Stable Macroevolutionary Inferences?
1176	An Example from Squamate Reptiles. Syst. Biol. 66:843–856. DOI: 10.1093/sysbio/syw102
1177	Togkousidis, A, Stamatakis A and Gascuel O. 2025. Accelerating Maximum Likelihood
1178	Phylogenetic Inference via Early Stopping to Evade (Over-)optimization. Syst. Biol.
1179	p.syaf043, DOI: 10.1093/sysbio/syaf043
1180	Torices R. 2010. Adding time-calibrated branch lengths to the Asteraceae supertree. J. Syst.
1101	Fig. 49:271 279 DOI: 10.1111/; 17F0.6921.2010.00099.v

1102	vianna JA, Fernandes FAN, Frugone WJ, Figueiro HV, Pertierra LK, Noii D, Bi K, Wang-Claypooi
1183	CY, Lowther A, Parker P, Le Bohec C, Bonadonna F, Wienecke B, Pistorius P, Steinfurth A,
1184	Burridge CP, Dantas GPM, Poulin E, Simison WB, Henderson J, Eizirik E, Nery MF, Bowie
1185	RCK. 2020. Genome-wide analyses reveal drivers of penguin diversification. Proc Natl Acad
1186	Sci USA 117:22303–22310. DOI: 10.1073/pnas.2006659117
1187	Vinay KL, Natesh M, Mehta P, Jayapal R, Mukherjee S, Robin VV. 2022. Re-assessing the
1188	phylogenetic status and evolutionary relationship of Forest Owlet (Athene blewitti (Hume
1189	1873)) using genomic data. Ibis 164:1278-1284. DOI: 10.1111/ibi.13097
1190	Wang N, Hosner PA, Liang B, Braun EL, Kimball RT. 2017. Historical relationships of three
1191	enigmatic phasianid genera (Aves: Galliformes) inferred using phylogenomic and
1192	mitogenomic data. Mol. Phylogenet. Evol. 109:217–225. DOI:
1193	10.1016/j.ympev.2017.01.006
1194	Wang Z, Zhang J, Xu X, Witt C, Deng Y, Chen G, Meng G, Feng S, Xu L, Szekely T, Zhang G, Zhou
1195	Q. 2022. Phylogeny and sex chromosome evolution of Palaeognathae. J. Genet. Genomics
1196	49:109–119. DOI: 10.1016/j.jgg.2021.06.013
1197	White ND, Braun MJ. 2019. Extracting phylogenetic signal from phylogenomic data: Higher-level
1198	relationships of the nightbirds (Strisores). Mol. Phylogenet. Evol. 141:106611. DOI:
1199	10.1016/j.ympev.2019.106611
1200	White ND, Mitter C, Braun MJ. 2017. Ultraconserved elements resolve the phylogeny of potoos
1201	(Aves: Nyctibiidae). J. Avian Biol. 48:872–880. DOI: 10.1111/jav.01313
1202	Wickham H. 2011. ggplot2. WIREs Comp Stat 3:180–185. DOI: 10.1002/wics.147
1203	Wilkinson M, Pisani D, Cotton JA, Corfe I. 2005. Measuring support and finding unsupported
1204	relationships in supertrees. Syst. Biol. 54:823–831. DOI: 10.1080/10635150590950362
1205	Winker K, Glenn TC, Faircloth BC. 2018. Ultraconserved elements (UCEs) illuminate the
1206	population genomics of a recent, high-latitude avian speciation event. PeerJ 6:e5735. DOI:
1207	10.7717/peerj.5735
1208	Wu S, Rheindt FE, Zhang J, Wang J, Zhang L, Quan C, Li Z, Wang M, Wu F, Qu Y, Edwards SV,
1209	Zhou Z, Liang L. 2024a. Genomes, fossils, and the concurrent rise of modern birds and
1210	flowering plants in the Late Cretaceous. Proc Natl Acad Sci USA 121:e2319696121. DOI:

1211	10.1073/pnas.2319696121
1212	Wu S, Rheindt FE, Zhang J, Wang J, Zhang L, Quan C, Li Z, Wang M, Wu F, Qu Y, Edwards SV,
1213	Zhou Z, Liang L. 2024b. Reply to Claramunt et al.: Robustness of the Cretaceous radiation of
1214	crown aves. Proc Natl Acad Sci USA 121:e2412448121. DOI: 10.1073/pnas.2412448121
1215	Xi Z, Liu L, Davis CC. 2016. The impact of missing data on species tree estimation. Mol. Biol.
1216	Evol. 33:838–860. DOI: 10.1093/molbev/msv266
1217	Yang Z, Rannala B. 2012. Molecular phylogenetics: principles and practice. Nat. Rev. Genet.
1218	13:303–314. DOI: 10.1038/nrg3186
1219	Yonezawa T, Segawa T, Mori H, Campos PF, Hongoh Y, Endo H, Akiyoshi A, Kohno N, Nishida S,
1220	Wu J, Jin H, Adachi J, Kishino H, Kurokawa K, Nogi Y, Tanabe H, Mukoyama H, Yoshida K,
1221	Rasoamiaramanana A, Yamagishi S, Hayashi Y, Yoshida A, Koike H, Akishinonomiya F,
1222	Willerslev E, Hasegawa M. Phylogenomics and morphology of extinct paleognaths reveal
1223	the origin and evolution of the ratites. Curr. Biol. 27:68–77. DOI:
1224	10.1016/j.cub.2016.10.029
1225	Younger JL, Strozier L, Maddox JD, Nyári ÁS, Bonfitto MT, Raherilalao MJ, Goodman SM, Reddy
1226	S. 2018. Hidden diversity of forest birds in Madagascar revealed using integrative
1227	taxonomy. Mol. Phylogenet. Evol. 124:16–26. DOI: 10.1016/j.ympev.2018.02.017
1228	Zarza E, Faircloth BC, Tsai WLE, Bryson RW, Klicka J, McCormack JE. 2016. Hidden histories of
1229	gene flow in highland birds revealed with genomic markers. Mol. Ecol. 25:5144–5157. DOI:
1230	10.1111/mec.13813
1231	Zhang C, Rabiee M, Sayyari E, Mirarab S. 2018. ASTRAL-III: Polynomial time species tree
1232	reconstruction from partially resolved gene trees. BMC Bioinformatics 19:153. DOI:
1233	10.1186/s12859-018-2129-y
1234	Zhang G, Li B, Li C, Gilbert MTP, Jarvis ED, Wang J, Avian Genome Consortium. 2014.
1235	Comparative genomic data of the Avian Phylogenomics Project. Gigascience 3:26. DOI:
1236	10.1186/2047-217X-3-26
1237	Zhao M, Kurtis SM, White ND, Moncrieff AE, Leite RN, Brumfield RT, Braun EL, Kimball RT. 2023.
1238	Exploring conflicts in whole genome phylogenetics: A case study within manakins (Aves:
1239	Pipridae). Syst. Biol. 72:161–178. DOI: 10.1093/sysbio/syac062

Zhao M, Oswald JA, Allen JM, Owens HL, Hosner PA, Guralnick RP, Braun EL, Kimball RT. 2025. A phylogenomic tree of wood-warblers (Aves: Parulidae): Dealing with good, bad, and ugly samples. Mol. Phylogenet. Evol. 202:108235. DOI: 10.1016/j.ympev.2024.108235

## 1245 Figure Legends

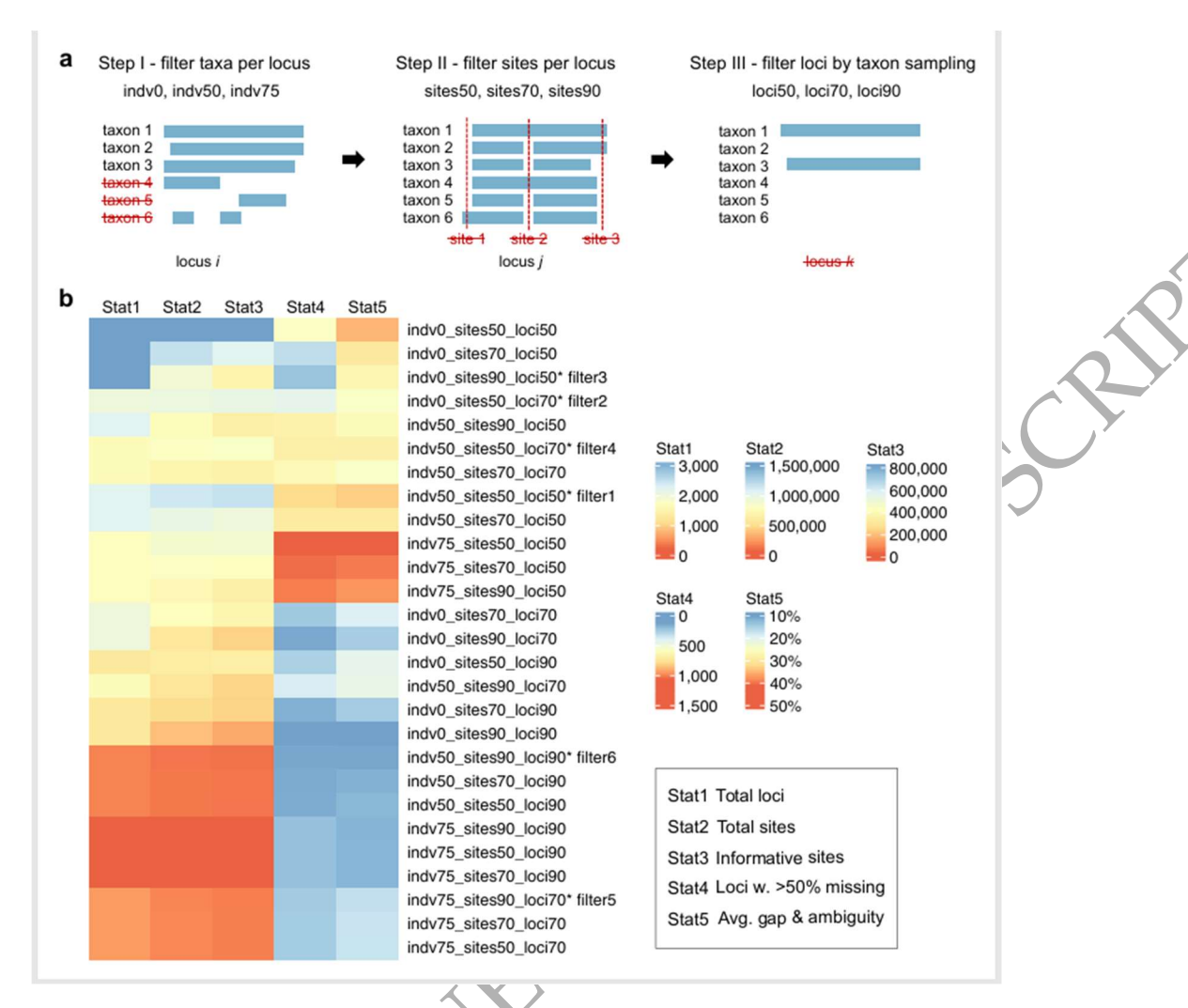
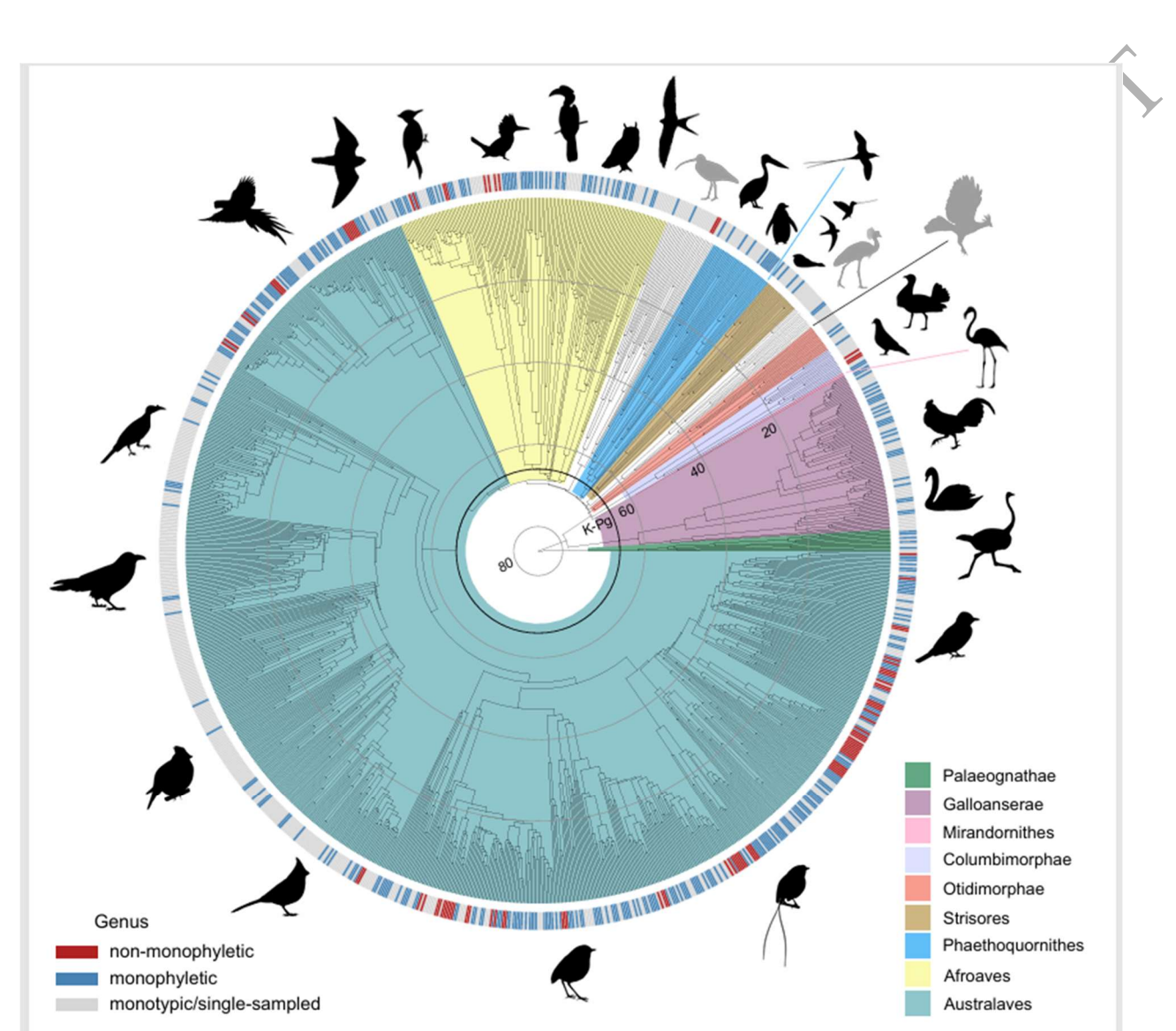


Figure 1. Filtering schemes and information content of different datasets. a) We used a combination of three strategies to filter datasets. Step I. Indv refers to the removal of individual taxa with short sequences for specific loci: indv0 indicates that we did not conduct this filtering step; indv50 and indv75 indicate that sequences shorter than 50% and 75% of the longest sequence for that alignment were removed. Step II. Sites refers to the trimming of sites dominated by gaps and missing data: sites50 indicates that alignment columns where ≥50% of taxa were gaps or missing are removed; sites70 and sites90 removed columns with ≥70% or ≥90% gaps or missing data, respectively. The percentage of taxa with gaps or missing data in a column reflects the number of taxa sampled for the locus of interest. Step III. Loci refers to the

removal of poorly sampled loci: loci50, loci70, and loci90 indicate that loci are retained only if they are sampled for  $\geq$ 50%,  $\geq$ 70%, and  $\geq$ 90% (respectively) of taxa in the full data matrix. b) Summary statistics (total number of loci, total number of sites, total number of parsimony informative sites, loci with > 50% data missing, and average proportion of gaps and ambiguities ["-", "?" and "N"] across all loci) of the sequence alignments in all 27 filtered datasets. For missing data information (Stat4 and Stat5), hotter colors represent more missing data.



**Figure 2**. A genus-level RAxML-NG tree with branch lengths converted to divergence time using TreePL. Major bird clades are color-coded, while three lineages (Gruiformes, Charadriiformes and Opisthocomiformes; see Reddy et al. 2017) that were not placed within a strongly

corroborated superordinal clade, remain uncolored (silhouettes in gray). Colored bars in the outer ring indicate genera that are monophyletic (blue; n = 372) and non-monophyletic (red; n = 38) in this phylogeny. Monotypic genera (n = 334 with a single species currently recognized in IOC World Bird List v13.1) and genera represented by a single sample in our dataset (n = 337) are gray. The concentric gray circles and adjacent integer values indicate 20 Ma time intervals. The black circle indicates the K-Pg boundary at 66 Ma. See Supplementary Figure S7 for a version of this tree with tip labels.

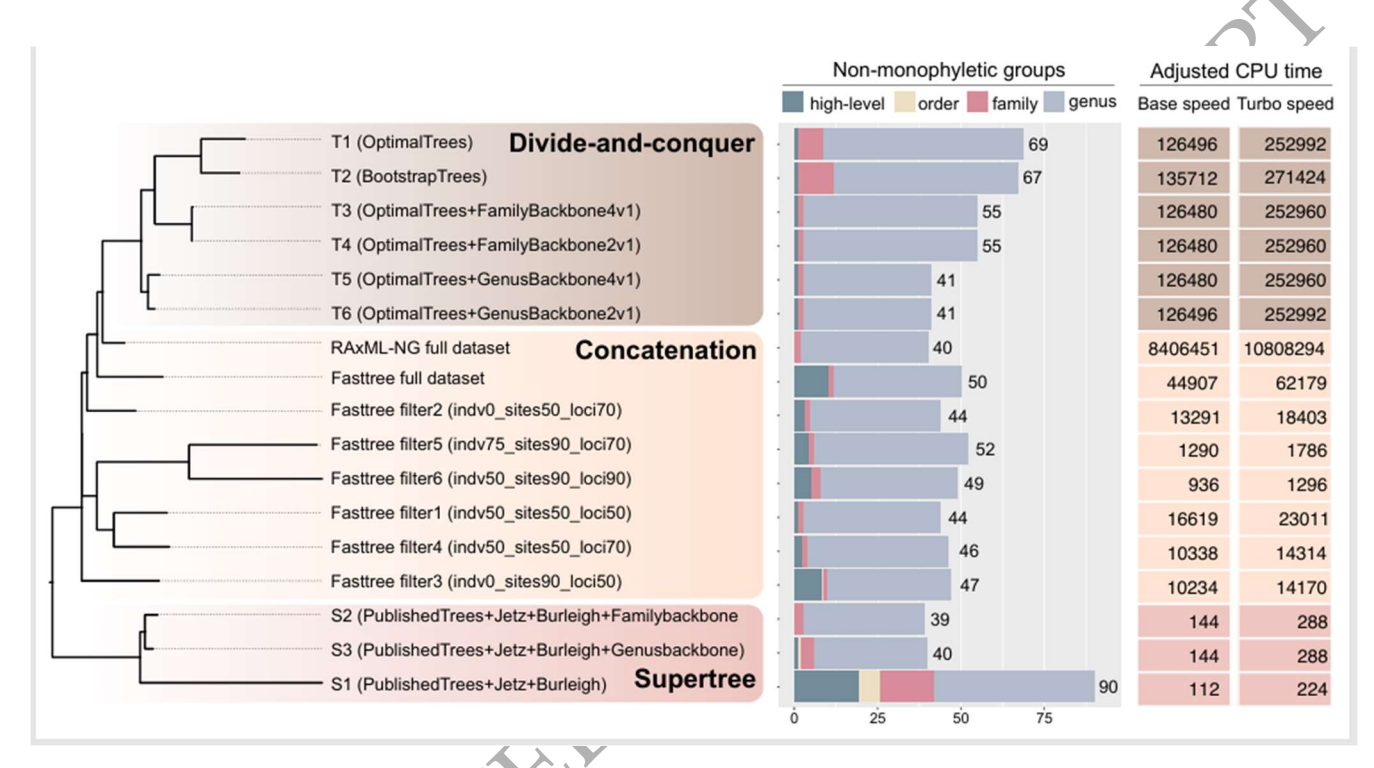
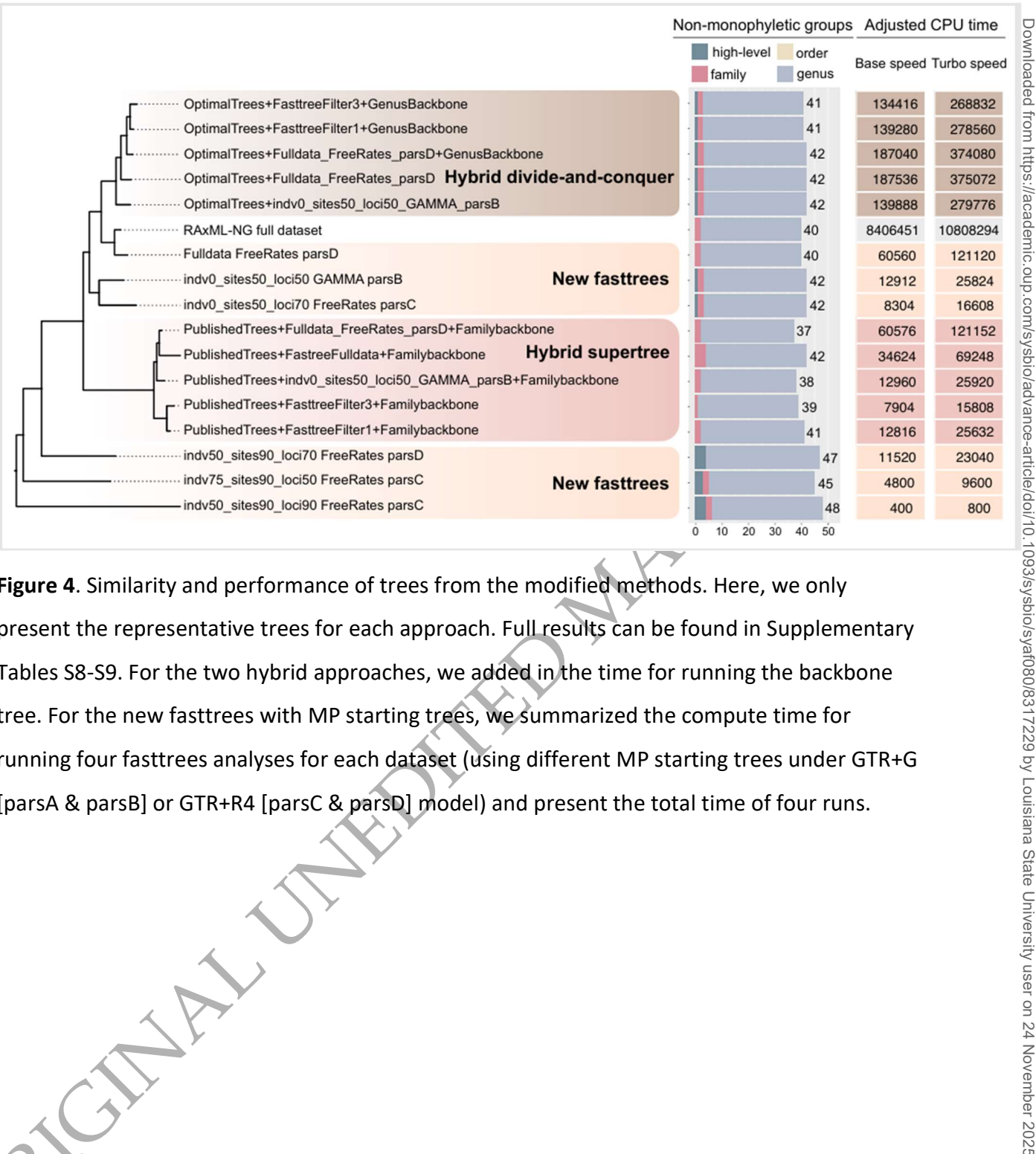


Figure 3. Similarity and performance of trees from the initial exploration. The phylogram represents tree similarity measured with normalized Robinson-Foulds distances and was constructed using neighbor-joining followed by midpoint rooting. ASTRAL results are not included but can be found in the Supplementary Table S11. For each tree, we summarized the number of high-level clades, orders, families, and genera recognized by IOC World Bird List v13.1 that are not monophyletic in the tree; therefore, the higher the number, the more non-monophyletic groups. Non-monophyly may be due to artifacts in phylogenetic inference or taxonomic classification that requires revision. The adjusted CPU time (CPU hours \* GFLOPS) required for each analysis is shown at the right (see Methods for details).



1287

1288

1289

1290

1296

1297

1298

1299

1300

1301

1302

1303

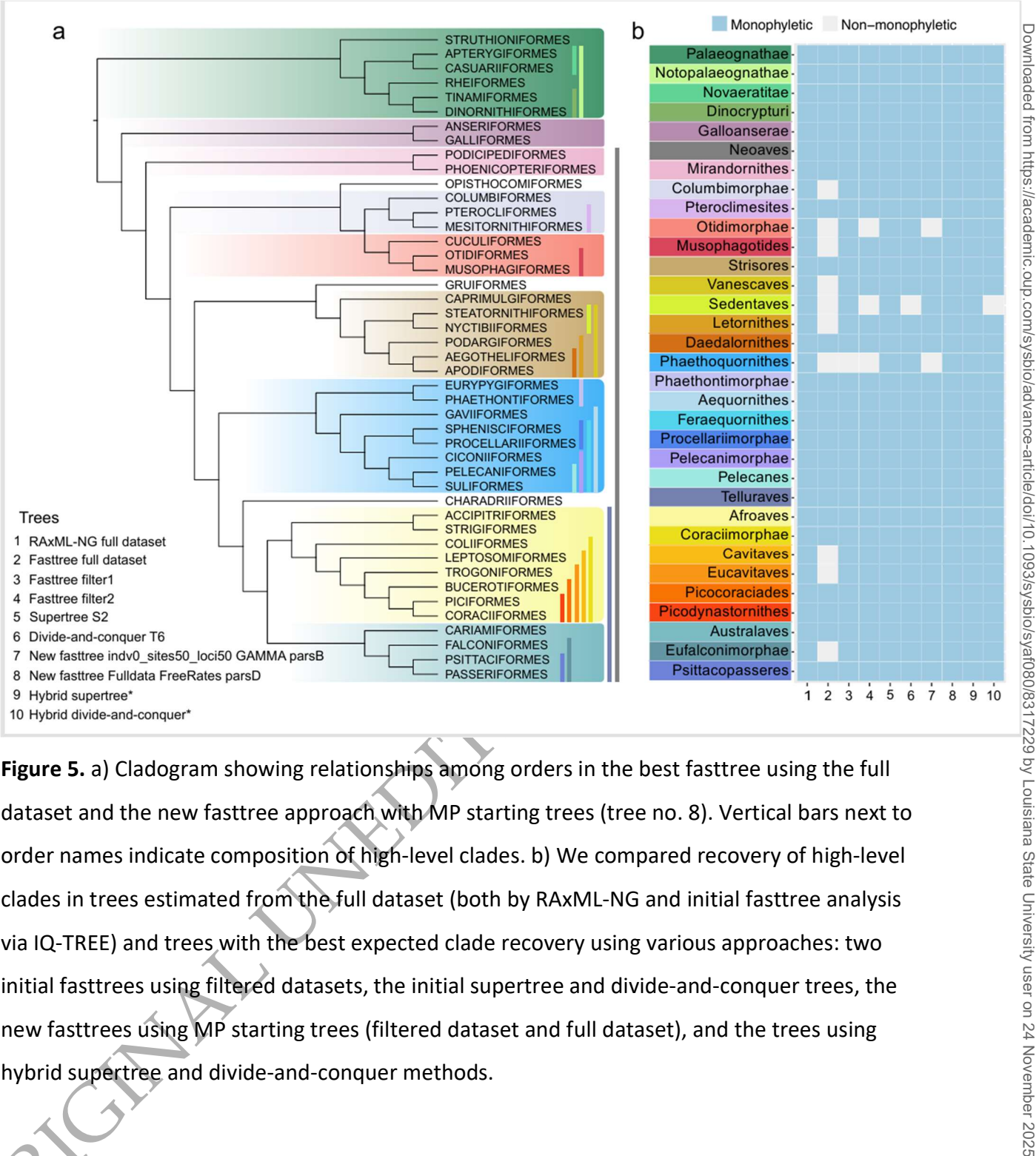
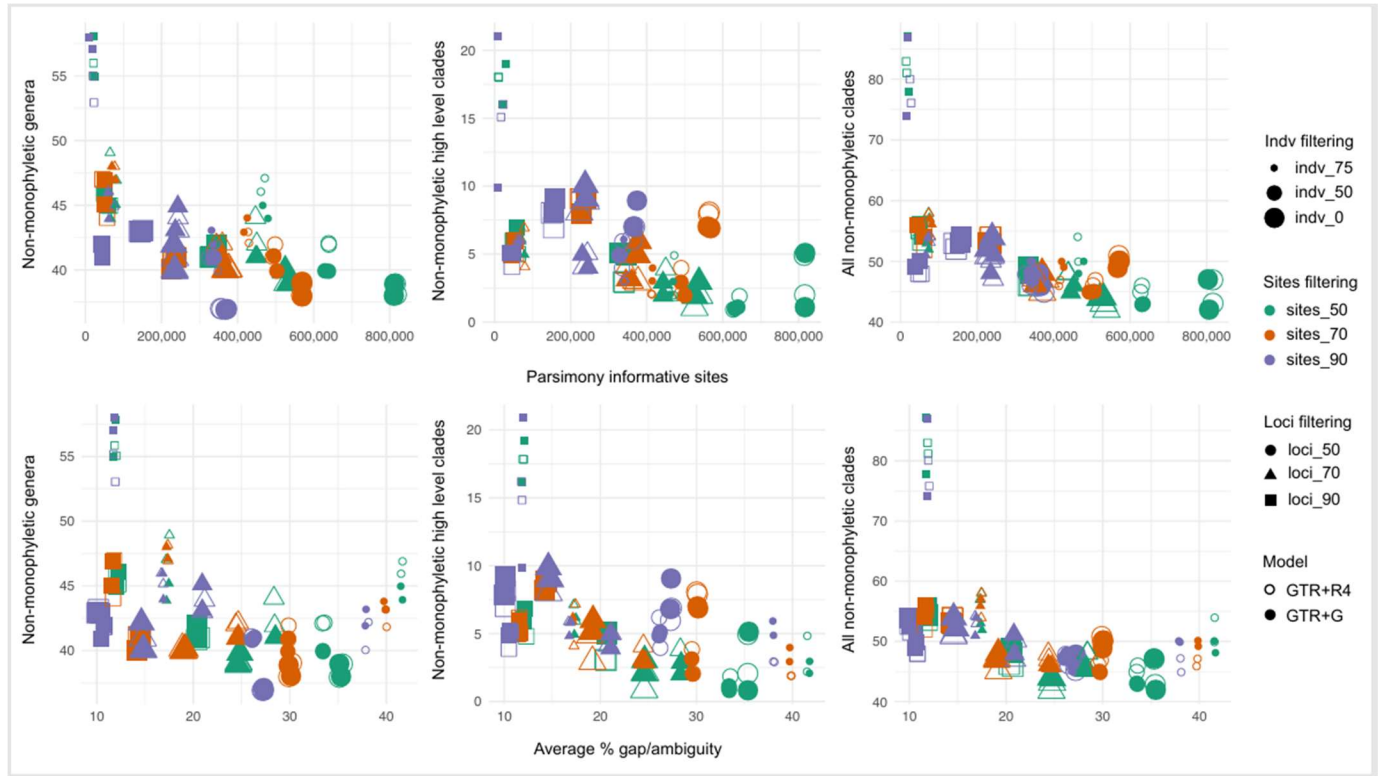
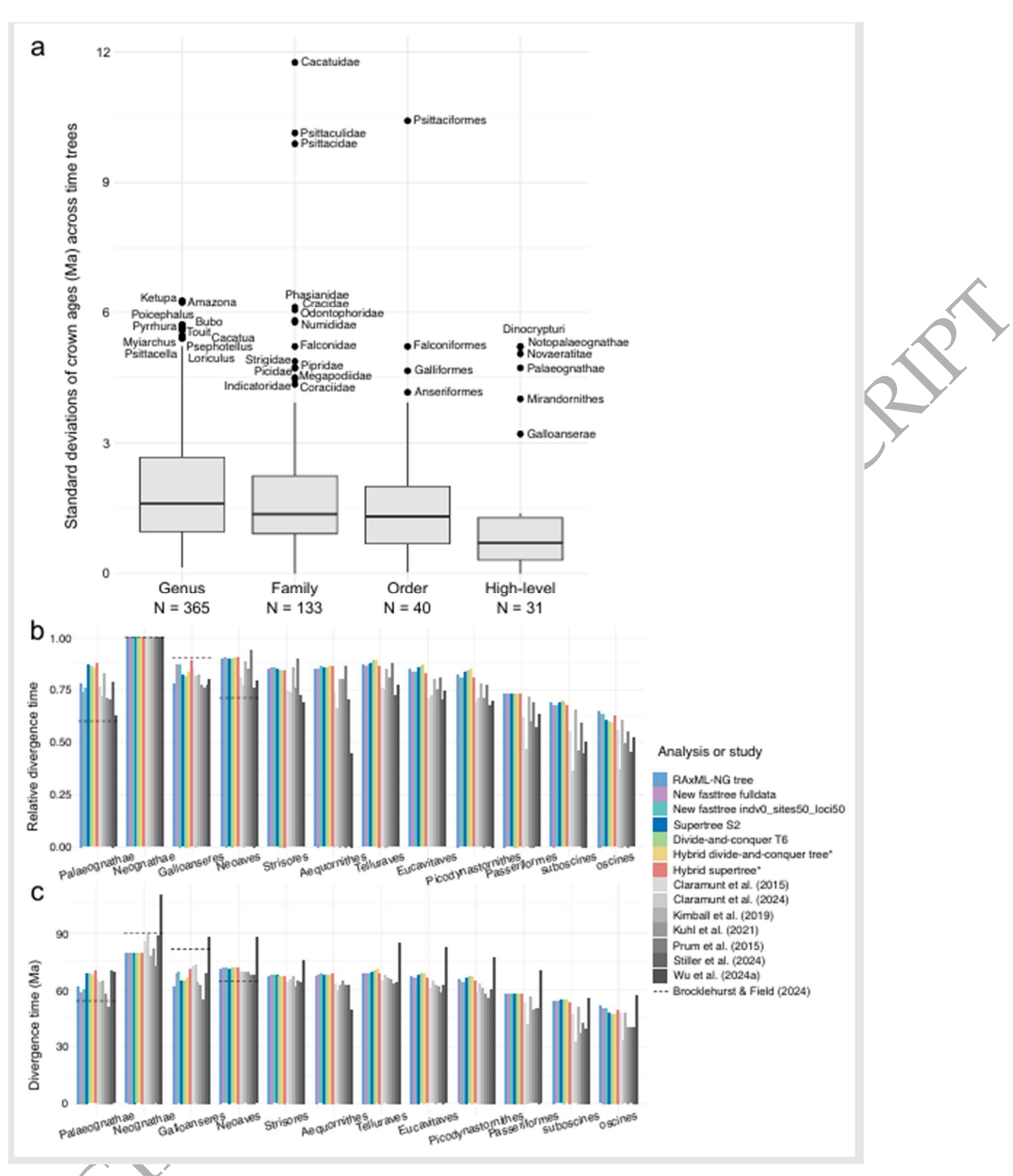


Figure 5. a) Cladogram showing relationships among orders in the best fasttree using the full dataset and the new fasttree approach with MP starting trees (tree no. 8). Vertical bars next to order names indicate composition of high-level clades. b) We compared recovery of high-level clades in trees estimated from the full dataset (both by RAxML-NG and initial fasttree analysis via IQ-TREE) and trees with the best expected clade recovery using various approaches: two initial fasttrees using filtered datasets, the initial supertree and divide-and-conquer trees, the new fasttrees using MP starting trees (filtered dataset and full dataset), and the trees using hybrid supertree and divide-and-conquer methods.



**Figure 6**. A comparison between the number of unresolved expected clades (genera, high-level clades, and all expected clades combined) and parsimony informative sites (top panels), as well as average proportion of gaps and ambiguities ("-", "?" or "N") across all locus alignments for the dataset (bottom panels). For each filtered dataset, four fasttrees with different parsimony starting trees were evaluated. We applied jitter to points when two shapes were completely overlapping so that both shapes would be visible.



**Figure 7.** Variation in estimated divergence times for different analyses. a) Standard deviations of crown ages (Ma) for evaluated clades in four ranks (genus, family, order and high-level clades) were calculated using our time trees. Only monophyletic groups were evaluated. The

plot of standard deviations shows their median, interquartile range (box), and 1.5x the interquartile range (whiskers). b) Crown ages for 12 major avian clades with relative divergence time (to Neognathae) for our time times. Crown ages from eight published time trees are included for comparison. c) Crown ages for 12 major avian clades shown as absolute divergence time.



**Table 1**. Summary of datasets, analyses, and phylogenetic trees in our initial exploration. The six filtered datasets were numbered based on total number of sites; filter1 included the highest number of sites and filter6 included the lowest number of sites.

METHOD	ANALYSIS	INPUT DATASET	TREE	
Supermatrix (baseline)	RAxML-NG	Full dataset	RAxML-NG full dataset	
Supermatrix (Strategy 1)	Fasttree via IQ-TREE	Full dataset	Fasttree full dataset	
		Filter1 (indv50_sites50_loci50)	Fasttree filter1	
		Filter2 (indv0_sites50_loci70)	Fasttree filter2	
		Filter3 (indv0_sites90_loci50)	Fasttree filter3	
		Filter4 (indv50_sites50_loci70)	Fasttree filter4	
		Filter5 (indv75_sites90_loci70)	Fasttree filter5	
		Filter6 (indv50_sites90_loci90)	Fasttree filter6	
Coalescent	Gene tree estimation	Full dataset	See Data	
species tree	via IQ-TREE	Filter1 (indv50_sites50_loci50)	Availability	
(Strategy 2)	&	Filter2 (indv0_sites50_loci70)	section	
	Gene tree summary via	Filter3 (indv0_sites90_loci50)	-	
	ASTRAL	Filter4 (indv50_sites50_loci70)	-	
		Filter5 (indv75_sites90_loci70)	-	
		Filter6 (indv50_sites90_loci90)	-	
Supertree (Strategy 3)	Without taxonomic backbone	PublishedTrees+Jetz+Burleigh	S1	
	Family backbone	PublishedTrees+Jetz+Burleigh+Familybackbone	S2	
	Genus backbone	PublishedTrees+Jetz+Burleigh+Genusbackbone	S3	
Divide-and-	Without backbone	OptimalTrees	T1	
conquer (Strategy 4)	Without backbone	BootstrapTrees	T2	
(ourategy 1)	Family backbone weighted 1:4	OptimalTrees+FamilyBackbone4:1	T3	
	Family backbone weighted 1:2	OptimalTrees+FamilyBackbone2:1	T4	
	Genus backbone weighted 1:4	OptimalTrees+GenusBackbone4:1	T5	
	Genus backbone weighted 1:2	OptimalTrees+GenusBackbone2:1	T6	

**Table 2**. Summary of datasets, analyses, and phylogenetic trees using modified methods.

METHOD	ANALYSIS	INPUT DATAS	ET		TREE
WEITIOD	AITALISIS	iiti o'i balasi	GTR+G	Replicates A,B	New fasttrees,
	Fasttree via IQ-	Full dataset		•	four for each
Fasttrees	TREE using		GTR+R4	Replicates C,D	dataset (GAMMA
with MP	parsimony starting		GTR+G	Replicates A,B	parsA, GAMMA
starting trees	trees estimated by	27 filtered	CTD - D4	Danlinston C.D.	parsB, FreeRates
	Parsimonator	datasets	GTR+R4	Replicates C,D	parsC, FreeRates
					parsD)
		PublishedTree	s + Fasttree Fu	lldata	Nine hybrid
		PublishedTree	s + Fasttree filt	ter1 – 6	supertrees with
	Include a fasttree	PublishedTree	s + Fulldata_Fr	eeRates_parsD	different fasttree
	backbone	PublishedTree	<u>s</u> +		as backbone,
		indv0_sites50	_loci50_GAMN	/IA_parsB	without
					taxonomic
		Dodeliele edTees	es + Fasttree Fu	U-l-+- ·	backbone
Hybrid				iidata +	
supertree		Familybackbo	es + Fasttree filt	tor1 _ 6 +	Nine hybrid
	Include a fasttree	Familybackbo		lei1-0+	supertrees with
	and a family			reeRates_parsD +	- different fasttree
	backbone		_	eenates_parsb +	plus a family-leve
	backbone	Familybackbo PublishedTree			<ul> <li>taxonomic tree as</li> </ul>
		indv0_sites50_loci50_GAMMA_parsB +			backbones
		Familybackbone			
		<u>_</u>	+ Fasttree Fullo	data	Nine hybrid
			+ Fasttree filte	7	, divide-and-
			+ Fulldata_Free		conquer trees
	Include a fasttree	OptimalTrees	_	·	with different
	as backbone		_loci50_GAMN	//A parsB	fasttree as
	as packbone	$\lambda \lambda Y$		<u>_</u> pao2	backbone,
					without
Hybrid					taxonomic
divide-and-		<i>&gt;</i>			backbone
conquer		•	+ Fasttree Full	data +	Nine hybrid
-1	<b>\</b>	GenusBackbo			- divide-and-
	Y	· ·	+ Fasttree filte	r1 – 6 +	conquer trees
	Include a fasttree	GenusBackbo			- with different
	and a genus	•	_	eRates_parsD +	fasttree plus a
	backbone	GenusBackbo			genus-level
( )	<b>Y</b>	OptimalTrees		44	taxonomic tree as
			_loci50_GAMN	/IA_parsB +	backbones
		GenusBackbo	ne		